

A UNIFIED APPROACH FOR MODELLING BJT BASED ON GUMMEL POON MODEL

By

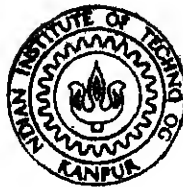
CHANDRASEKHAR MUKHERJEE

EE

Thesis
621 38832
M8964

1986

M
MUK
UNI



DEPARTMENT OF ELECTRICAL ENGINEERING
INDIAN INSTITUTE OF TECHNOLOGY KANPUR
JUNE 1986

221 38 2
- 18362

23 EP 1987
CENTIF H 5-18

A No A 980 1 1

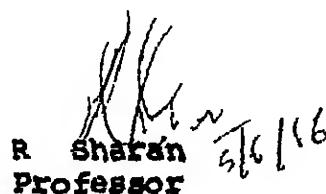
EE 1100 M-MUK UNI

CERTIFICATE

This is to certify that the thesis entitled
A UNIFIED APPROACH FOR MODELLING BJT BASED ON GUMMEL POON
MODEL by Chandrasekhar Mukherjee has been carried out under
our supervision and that it has not been submitted elsewhere
for a degree



R Raghuram
Assistant Professor


5/6/16

R Sharan
Professor

Department of Electrical Engineering
Indian Institute of Technology
Kanpur 208016 INDIA

ACKNOWLEDGEMENTS

I wish to take this opportunity to express my deepest sense of gratitude to my supervisors Dr R Sharan and Dr R Raghuram for suggesting me this interesting problem. I am greatly indebted to them for their sincerest advice, inspiration and constructive criticism during the course of the work.

My sincerest thanks are also due to those innumerable friends who made my stay memorable one.

Finally, I deeply appreciate the remarkable typing done by Mr R N Srivastava and the neat tracing by Mr J C Verma.

-CHANDRASEKHAR MUKHERJEE

CONTENTS

	<u>Page</u>
CHAPTER 1 INTRODUCTION	1
1 1 Concept of modelling	1
1 2 Aim of the work	2
1 3 Organisation of the thesis	2
CHAPTER 2 GUMMEL POON MODEL	4
2 1 Introduction	4
2 2 1 Basic derivation of G-P model equation	5
2 2 2 Approach in modelling	9
2 3 Nonlinear effects	14
2 3 1 Early effect	15
2 3 2 Mobility variation in the base region	22
2 3 3 Variation of τ_f and τ_r with I_c	24
2 4 High injection effects	34
2 4 1 Conductivity modulation in the base	34
2 4 2 Base push out effect	39
2 4 3 Quasi saturation region in the collector	43
2 5 Emitter region solution	48
2 6 Edge crowding effect	49
2 7 Parasitic effects	62
2 8 Summary	67
CHAPTER 3 TRANSISTOR CURVE TRACER	68
3 1 Introduction	68
3 2 Basic building block	68
3 3 1 Collector sweep circuit	71
3 3 2 Measurement section	75
3 4 Base step generator	77
3 4 1 Synchroniser and frequency multiplier	77
3 4 2 Triangular/sweep generator	81
3 5 Conclusion	85

CHAPTER	4	FORMULATION OF THE MODEL	87
	4 1	Introduct on	87
	4 2	Model equations electrical measurements and extra tion of model parameters	89
	4 2 1	C_e as a function of V_{BE} and C_c as or function of V_{BC}	90
	4 2 2	h_{FE} versus I_c (at low injection)	91
	4 2 3	Measurement of emitter and collector series resistances	93
	4 2 4	I_c as a function of V_{BE} at constant V_{CE}	94
	4 2 5	Output characteristics (V_{CE} versus I_c) in saturation region	95
	4 2 6	f_T as function of I_c at constant V_{CE}	96
	4 3	Modelling on the basis of extended GP model	104
	4 3 1	Extraction of parameters on base push out effect	108
	4 4	Comparison with SPICE model	109
CHAPTER	5	SOFTWARE DEVELOPMENT	111
	5 1	Introduction	111
	5 2	Objective functions	111
	5 3	Results and discussions	117
CHAPTER	6	CONCLUSION AND SCOPE FOR FURTHER WORK	124
REFERENCES			126
APPENDIX I		Balancing techniques of offset of opamps	
APPENDIX II		Collector base junction width as a function of voltage	

APPENDIX III	List of parameters adopted in SPICE and in our model
APPENDIX IV	Flow chart of the software package
APPENDIX V	Levenberg Marquasdt Algorithm

ABSTRACT

In this thesis entitled A UNIFIED APPROACH FOR MODELLING BJT BASED ON GUMMEL POON MODEL a set of parameters related by a set of model equations has been postulated which specify transistor electrical behaviours for all regions of its operation

The device model chosen is based on Gummel-Poon charge control model Extensions/modifications are made wherever necessary Help is taken from some recent techniques reported for modelling nonlinear effects that occurs inside a transistor In the remaining cases we have made our own derivations and also that required to accommodate various nonlinear effects occurring simultaneously

The parameters are extracted using nonlinear least square curve fitting algorithm suggested by Levenberg-Marquardt The data points are obtained from the experimentally observed characteristic curves of the transistor To take measurement a precision curve tracer is built as a part of the project work

The parameters chosen are physical parameters and their relationship with device material and structural parameters are indicated These relationships can be utilised for checking the validity of the model

Finally comparison between the proposed model and existing SPICE model is made

CHAPTER 1

INTRODUCTION

1.1 THE CONCEPT OF MODELLING

The term model has a number of overlapping meanings which can easily create confusion. The most common meaning encountered is the reference to the simulation of the physical appearance of an object generally on a different physical scale. A more relevant meaning for our purpose is the duplication of its physical appearance. One then can construct a set of equations (i.e. a mathematical model) to portray the internal behaviour as well as that with the surroundings. A still more robust meaning has to do with the as if analysis of the system. By noting some external behaviour using perturbation one replaces the system (a black box) by a set of interacting elements with known behaviour. This conceptualized (as opposed to constructed) model presents circumstances with known principles which acts as a generator of principles in the theorist thinking. The laws or operating principles in the model postulated are assumed to hold good for the system. The laws for the system being so modelled constitutes the theory. It is also possible to go further and assume that the physical constitution of the unknown circumstances requiring a theory is similar to that of the model (viz. the hybrid model of a transistor). The use of either hypothetical systems or analogous physical systems allows for rich conjecture which

in turn allows more powerful theories to emerge. The analogy of the physical model builds the theory for the model or if the theorist recognizes that he has only a partial analogy in his model the model at least contributes some axioms to his theory (e.g. the example cited above)

1.2 AIM OF THE WORK

It is also possible to build theories as opposed to conceptual or physical models and still obtain some end result. But the advantage of models is that they usually make theoretical development easier. Though the simulation based on Gummel Poon model in its early days has incorporated both physical and conceptual theories with more and more understanding of the behaviour of a transistor available nowadays it is possible to reformulate the model fully based on physical theories. The aim of this work is towards this line. Of course prior validation of the theory and the verification of the software package are mandatory before one can use it to study or simulate larger systems. There are various levels of modelling we have more to say about this in Chapter 4.

1.3 ORGANISATION OF THE THESIS

The structure of this thesis is as follows. In Chapter 2 we have started with the Gummel Poon model the focus of the work. Later on various auxiliary effects that significantly affect the functioning of the transistor are discussed. Some more parameters are also included to consider some new effects which are not taken care of in the Gummel Poon

model initially proposed. We have also replaced some of the old theories by new theories recently developed by others or by us. In Chapter 3 we have gone to develop a curve tracer to take measurements required for the evaluation of the model parameters. In Chapter 4 in the introductory part we have reiterated the concept of modelling with its relevance to our work. In Section 4.2 we have made a systematic discussion about how we can find out the parameters from some typical measurements whereas in the very next section we have hinted about the salient points in our proposed model. Finally we have indicated the compatibility of ours with the SPICE model and merits/demerits between them.

CHAPTER 2

GUMMEL POON MODEL

2.1 INTRODUCTION

Any model on bipolar junction transistors must reflect the fact that a transistor consists of two p-n junctions. The simplest yet novel version of it is the Ebers-Moll model [6] where the two junctions are represented by ideal exponential functions relating current and voltages. This model embodies superposition that is that the transported current from emitter to the collector can be expressed as a sum of two independent components resulting from the biasing of the junctions or the junctions act independently. For real transistors the violation of superposition principle is easily observed for example the Early effect [37] denotes the dependence of low frequency output conductance on bias. For a transistor operating in its active region (Figure 2.1(d)) the collector current I_C is seen to increase slowly with collector-emitter voltage V_{CE} . This is due to base width modulation by the collector-base bias voltage. Ebers-Moll's model is unable to include this and other second order effects like high injection effects, bias dependent current gain. An improvement in this respect is achieved by the Gummel-Poon Model [7] based on charge control theory, an extension on Moll-Ross version [8]. Uptil now Gummel-Poon model is widely accepted for designing transistors as it is capable of describing the second order effects (just mentioned above).

more or less accurately. However we will show in our work this model is still capable of handling some other important effects like conductivity modulation in the base and in the low-doped collector regions emitter crowding etc

Since our work is basically based on this model we will first describe it in detail. Side by side we will point out the approximations taken at different stages and their validity for various region of operation of transistors. Thereafter we will pass on to derivation of base-transit time as a function of current, minority carrier charges in the base region and finally emitter crowding effect.

2.2.1 BASIC DERIVATION OF G-P MODEL EQUATION

At any point in a semiconductor electron and hole current densities j_n and j_p are related to the carrier concentrations by the expression

$$\vec{j}_n = q \mu_n n \vec{E} + q D_n \vec{\nabla} n \quad (2.1)$$

and
$$\vec{j}_p = q \mu_p p \vec{E} - q D_p \vec{\nabla} p$$

Multiplying the first one by μ_p and the second one by μ_n and then subtracting so as to eliminate \vec{E} we end up with

$$\mu_p p \vec{j}_n - \mu_n n \vec{j}_p = \mu_n \mu_p kT \vec{\nabla} (np) \quad (2.2)$$

where Einstein's relation $D = \mu kT/q$ for either type of carriers is assumed. This expression is quite general and in one dimensional form it reduces to

$$\mu_p p j_n - \mu_n n j_p = \mu_n \mu_p kT \frac{d}{dx} (np) \quad (2.2)$$

Let us apply this result in the base region of a transistor. Gummel has assumed the base current to be negligible i.e. unit emitter efficiency and no recombination. With this assumption $j_p \approx 0$ and $j_n = \text{const} = j_{cc}$ (called the transported current) and equation (2.2a) becomes

$$p j_{cc} = \mu_n kT \frac{d}{dx} (np) \quad (2.3)$$

Integrating this expression from x_E the edge of the base depletion layer on the emitter end to $x = x_C$ the edge of the depletion region on the collector end we get

$$\int_{x_E}^{x_C} \frac{p j_{cc}}{\mu_n} dx = kT(n_E p_E - n_C p_C) \quad (2.4)$$

where suffix E and C is related to quantities at the emitter and collector junctions respectively. If we now use the junction law relating charge densities with junction voltages as

$$n_E p_E = n_i^2 e^{V_{BE}/V_T} \quad \text{and} \quad n_C p_C = n_i^2 e^{V_{BC}/V_T} \quad (2.5)$$

We will arrive at

$$j_{cc} = kT n_i^2 \frac{e^{V_{BE}/V_T} - e^{V_{BC}/V_T}}{\int_{x_E}^{x_C} p dx / \mu_n} \quad (2.6)$$

which is the Gummel equation. The prime sign is used with the junction voltages so as to differentiate from measured voltages. If we neglect position dependent mobility the

denominator of (2.6) can be replaced by the $\mu_n Q_B$ where Q_B is the majority carrier sheet charge density in the base region. On further defining the following relationship

$$\begin{aligned} I_{CC} &= -A_e J_{CC} \\ Q_b &= A_e Q_B \\ I_s &= \frac{q^2 D_n n_1^2}{Q_{bo}} A_e^2 \end{aligned} \quad (2.7)$$

where A_e is the emitter area; from (2.6) the expression for current density can then be changed over to an expression for linking current I_{CC} as

$$I_{CC} = I_s \left(\frac{Q_{bo}}{Q_b} \right) (e^{V_{BE}/V_T} - e^{V_{BC}/V_T}) \quad (2.8)$$

The same expression is derived by Gummel [31] in a somewhat different fashion. Here Q_{bo} stands for the doped charge in the quasi neutral active base region when no h is applied and the quantity I_s is called the saturation current of the transistor.

From the modelling point of view two important features should be noted which show the novelty of the G-P model. Firstly the rapidly varying exponential factors e^{V_{BE}/V_T} and e^{V_{BC}/V_T} appear explicitly in the numerator of equation (2.8). These factors do not depend on any model parameter (whereas in the E-M model the exponential terms depend on emission coefficients which are experimentally

determined model parameters) Thus when the junction voltages are known they can be evaluated accurately The remaining variable in (2 8) is the total mobile charge Q_b in the base region which is more slowly varying function of bias than the exponentials in the numerator This leads to second important feature of this new charge control relation modelling of the bias dependence of the Q_b There is a great deal of flexibility involved in the modelling of Q_b Trade offs are possible between complexity and accuracy In their original paper [7] Gummel-Poon writes Q_b as the sum of the doped charge in the effective base region and the excess majority carrier charge The latter ^{is} equated with injected minority carrier charge by assuming quasi neutrality condition ($n_e(x) = p_e(x)$) It is further related to forward and reverse currents via charge control theory The break up is as follows

$$\begin{aligned}
 Q_b &= q A_e \int_{x_E}^{x_C} (N_A(x) + n_e(x)) dx \\
 &= q A_e \int_{x_E}^{x_C} N_A(x) dx + \int_{x_E}^{x_C} n_e(x) dx \\
 &= Q_{b0} + Q_{be} + Q_{bc} + B \tau_f I_f + \tau_r I_r
 \end{aligned} \tag{2 9}$$

The first term in the expansion represents the base charge at zero bias Q_{be} Q_{bc} represent the increase/decrease of base charge because of reduction/extension of depletion region in the base under the application of bias voltage in

BE and BC junctions respectively. Their values are positive for positive bias and negative for negative bias in npn transistor. The fourth and fifth terms represent the injected charge from the emitter and collector junction respectively. In deducing this the so-called charge control principle is used which says that a stored charge Q is proportional to the related current I ($Q = \tau I$) where τ has the physical significance of the transit time. Thus τ_f and τ_r represent the forward and reverse transit times where I_f and I_r denote the forward and reverse currents. In the fourth term the factor B is introduced in order to tackle base push out effect. We will elaborate this point later on.

2.2.2 Approach in Modelling

Let us now look in detail the intrinsic operation of a transistor. In Figure 2.1 is shown a schematic side view of a discrete n-p-n transistor along with the flow of electron and hole currents. The solid line represents the flow of electrons and the dashed line represents the flow of holes. The superscript e and n are to distinguish particle current symbols. The collector current I_c consists of four components

$$I_c = I_{cc} - I_{bc1} - I_{bc2} + I_A \quad (2.10)$$

where I_{cc} is the dominated collector current through the transistor and its bias dependence is given in (2.8). It represents the injection of electrons from the emitter into the base which traverse the base region (by diffusion and partly by drift when base grading is present) and ultimately collect,

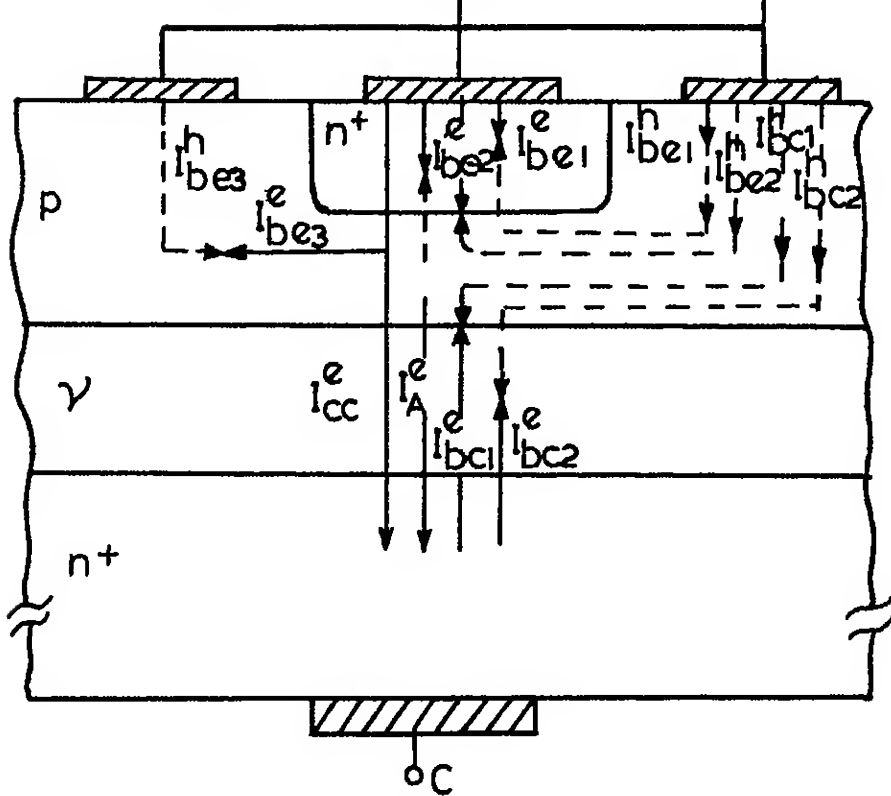


Fig 21 Schematic cross section of a transistor (not to the scale) showing various current components

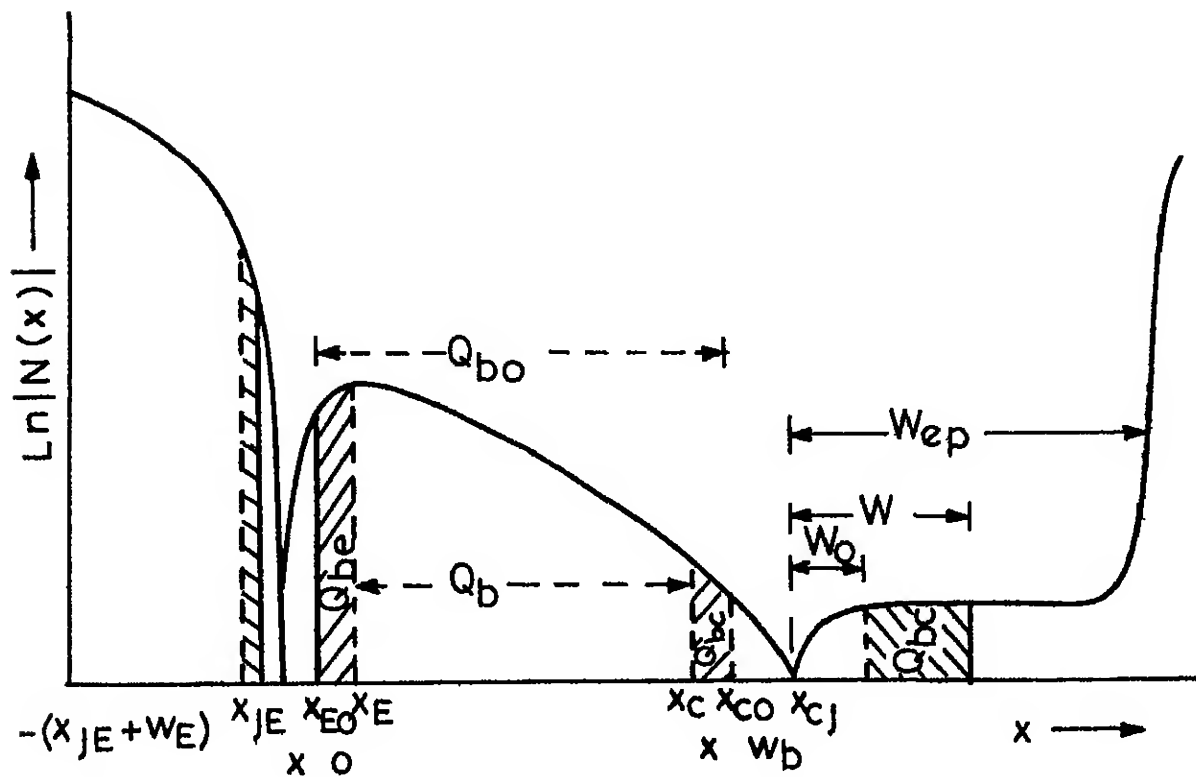


Fig 22 Typical impurity profile for an epitaxial transistor showing charges associated with various regions

at the collector I_{bc1} and I_{bc2} are the small components due to recombination in the collector-base junction depletion region and in the bulk I_A is the current component generated by impact ionization. Electrons generated by impact ionisation flow into the collector and become an additional current component to the collector current. For a transistor biased in the active region I_{CC} is generally much larger than the other three. The current I_A is in fact important only at high CB junction reverse voltages. Since we are not interested in high voltage operation we will neglect its presence all throughout. Modelling impact ionisation is a separate issue and we refer to [8 9]

I_{CC} comprises of two parts I_f and I_r already introduced in (2 9). I_f represents a forward injected current due to electrons injected from emitter to the base (for an npn transistor). I_r is the inverse electron current due to electron injection from collector to the base. They can be expressed as

$$I_f = \frac{I_s Q_{bo}}{Q_b} (e^{V_{BE}/V_T} - 1) \quad (2.11)$$

$$I_r = \frac{I_s Q_{bo}}{Q_b} (e^{V_{BC}/V_T} - 1)$$

Implicit is the assumption of reciprocity theorem which is valid under reasonable conditions. Thus

$$I_{CC} = I_f - I_r \quad (2.12)$$

The total recombination rate is modelled phenomenologically and consists of five components two ideal and three non-ideal. In absence of I_A this also equals the base current I_b given by

$$I_b = I_{be1} + I_{be2} + I_{be3} + I_{bc1} + I_{bc2} \quad (2.13)$$

I_{be1} represents the holes coming in from the base contact that are injected into the emitter region. These holes recombine in the bulk emitter region as shown in Figure 2.1. Thus I_{be1} has the ideal exponential dependence on V_{BE} of the form

$$I_{be1} = \frac{I_s}{\beta_F} (\exp(V_{BE}/V_T) - 1) \quad (2.14)$$

where β_F is called forward amplification factor. This definition is justified at low injection active region whence $Q_b = Q_{b0}$ and if one neglects the recombination generation current then this factor stands for the ratio I_C/I_B and is related to device parameter by

$$\beta_F = \frac{A_e q D_n N_E l_E}{Q_{b0} D_p \coth(W_E/l_E)} \quad (2.14')$$

here l_E , W_E , N_E stands for diffusion length, depth and doping density in the emitter region respectively.

I_{be2} represents holes injected from the base contact which recombine in the emitter junction. It can be modelled as

$$I_{be2} = I_{se} (e^{V_{BE}/n_e V_T} - 1) \quad (2.15)$$

Here I_{SE} is called space charge limited saturation current and n_e is a constant whose value lies between 1 and 2. An approximate expression for I_{SE} is

$$I_{SE} = q A_e n_i V_T / 2 \tau E_{max} \quad (2.15a)$$

where τ is the life time of electron or hole in the depletion region and E_{max} is given by

$$E_{max} = \left[\frac{2q N_A(x_E) N_E (V_{BIE} - V_{BE})}{\epsilon (N_A(x_E) + N_E)} \right]^{1/2} \quad (2.15b)$$

where V_{BIE} = built in voltage $N_A(x_E)$ is the doping level at the edge of the depletion region in the base. Needless to say these quantities are related to EB junction.

The third component of (2.13) takes care of recombination in the bulk region of the base. Using charge control theory it can be modelled as

$$I_{be3} \cong \frac{Q_b - Q_{b0}}{\tau_b} \quad (2.16)$$

where τ_b is the recombination life time in the base region. Using (2.9) we see that $I_{be3} \cong (\tau_f / \tau_b) I_C$ (roughly). In modern days planar transistor having narrow base width this ratio is quite small and one may neglect it as well.

The last two contributors to I_b considered in (2.13) comes from holes injected from the base contact which recombine in the collector epilayer and junction regions. As in (2.14) and (2.15) we can similarly model them:

$$I_{bc1} = I_s / \beta_R (e^{V_{BC}/V_T} - 1) \quad (2.17)$$

and

$$I_{bc2} = I_{SC} (e^{V_{BC}/n_e V_T} - 1) \quad (2.17a)$$

Here β_R is the reverse amplification factor I_{SC} is reverse saturation leakage current. They can be attributed similar theoretical expressions as in (2.14a) and (2.15a) with the only difference is that the suffixes related to EB junction have to be replaced by that of collector base junction.

It is to be noted that in equation (2.13) we have not considered contribution from overlap diode comprising of

inactive area of the CB junction. This is important when CB junction is forward biased and we will consider it later or (Sec 2.7). Equations (2.8), (2.9) and (2.13) summarize the basic equations that describe the intrinsic part of the transistor. A similar description is possible for pnp transistor also.

2.3 NONLINEAR EFFECTS

The nonlinearity of a transistor as it appears in the basic E-M model via the exponential form of the junction voltages in a way does not violate superposition as the currents derived from them are independent of the other. But in a real transistor many secondary effects arise. They are listed as follows: 1) Early effect, 2) conductivity modulation in the base and collector epitaxial region, 3) base push out effect, 4) emitter or edge crowding, 5) degeneracy in the emitter region, 6) voltage dependence of junction capacitances, 7) impact ionization, 8) surface leakage currents and parasitics. Apart from these some physical phenomena like band gap narrowing, mobility behaviour of minority carriers, gradin

of doping concentration in the emitter and base region variation of transit time with current density etc to some extent impress on the functioning of a transistor some of which we will also take care of In the above list we will set aside the seventh one as it is important only at very high reverse junction voltage and we rather refer to [8 9] Let us discuss these effects critically in the light of G-P model and modifications are suggested wherever necessary

2 3 1 Early Effect

The Early effect [37 17 20] arises because of the change in the effective base width as the collector-base junction width changes This effective decrease of base width (for reverse bias) reduces the recombination rate in the base region (and hence improvement in transport factor) and more importantly enhances the diffusion current because of sharper minority carrier gradient in the base region From a charge control point of view changes in Q_C the charge capacitively stored in the collector base junction cause changes in the collector current This give rise to an output conductance approximately given by

$$g_{out} = \frac{I_C^0 C_C}{Q_{bo}} \quad (2.18)$$

where I_C^0 is the collector current if there were no Early effect C_C CB junction capacitance

The conventional junction capacitance is related to junction voltage through an expression containing three parameters

$$C = \frac{C_{oe}}{(1 - v/v_{bi})^m} \quad (2.19)$$

The parameters are v_{bi} junction built-in voltage (typically ~ 0.7 V for Si) the grading coefficient m the constant in the numerator which can be related to the zero bias capacitance. But this expression suffers from numerical instability as v approaches v_{bi} C goes to infinity. In a real transistor of course a finite amount of charge is stored for all bias conditions and the derivatives of charge with respect to junction voltage is finite. In order to avert this problem Gummel has introduced a fourth parameter in the denominator of (2.19). They have defined a function [39]

$$f(v, P) = p_3 \frac{1}{(1 + p_4)^{p_2}} + \frac{v/p_1 - 1}{[(v/p_1 - 1)^2 + p_4]^{p_2}} \quad (2.19a)$$

where the vector P denotes the four parameters p_1 , p_2 , p_3 and p_4 in brevity. The normalised emitter and collector charges are then given by

$$q_{be} = f\left(\frac{qV_{BE}}{V_T}, P_e\right) \quad (2.20)$$

$$q_{bc} = f\left(\frac{qV_{BC}}{V_T}, P_c\right) \quad (2.21)$$

Though our software is based on this model concept a few points should be brought in before we pass on to the next topics. Because of the complex nature of the function (2.19) the parameters are not readily amenable to numerical evaluation.

Further in deriving these expressions the nature of the doping profile at the junction is not considered and the expression for CB and EB junction comes under the same token since they are purely model parameters they are not as such directly related to device design parameters. Hence evaluation of them does not provide any significant feedback to the designer. So to be realistic we prefer to present here two different approaches. The first one is due to us and the last one is somewhat close to the prescription [20].

In Figure 2.2 is shown the doping profile and charge associated with various regions commensurate with our definition. The points x_{jE} and x_{jC} specify the metallurgical junctions. The points x_{EO} and x_{jO} represent the edges of depletion layers in the base when no bias is applied. The points x_E and x_C show the same under a typical operating situation of the transistor. So according to our definition

$$\begin{aligned}
 Q_{bo} &= A_e q \int_{x_{EO}=0}^{x_{CO}} N_A(x) dx \\
 Q_{be} &= A_e q \int_{x_{EO}=0}^{x_E} N_A(x) dx \\
 Q_{bc} &= A_e q \int_{x_{CO}}^{x_C} N_A(x) dx
 \end{aligned} \tag{2.22}$$

Let us assume doping profile in the base region as

$$N_A(x) = \hat{N}_A e^{-C_F x} \quad \text{for } 0 \leq x \leq x_{jC}$$

$$\wedge -C |x|$$
(2.22b)

where C_F and C_R can be called forward and reverse grading coefficient in the base. They are both positive and their value can be approximated by

$$C_F = \frac{\ln N_A / N_A(x_{CO})}{w_b}$$

$$C_R = \frac{\ln \hat{N}_A}{x_{jE}}$$
(2 22b)

We now can get closed form expression for Q_{bo} , Q_{bc} and Q_{be} . From (2 22) and (2 22a)

$$Q_{bo} = q \hat{N}_A A_e (1 - e^{-C_F w_b})$$

$$Q_{bc} = q \hat{N}_A A_e (e^{-C_F x_C} - e^{-C_F w_b})$$

$$Q_{be} = q \hat{N}_A A_e (1 - e^{-C_R |x_E|})$$
(2 22c)

This is the situation in forward injection. For reverse injection with EB in reverse biased, only the expression for Q_{be} ought to be changed by simply replacing C_R by C_F . In normalised form

$$q_{bc} = \frac{Q_{bc}}{Q_{bo}} = \frac{(e^{C_F x_C} - 1)}{(e^{C_F w_b} - 1)}$$

$$q_{be} = \frac{Q_{be}}{Q_{bo}} = \frac{1 - e^{-C_R |x_E|}}{1 - e^{-C_F w_b}}$$
(2 22d)

To relate these quantities with junction voltages is a fairly involved task (see Appendix II). But this can be easily

computed from the constant collector epi-profile if we suppose an abrupt space charge region with identical amount of opposite charges on the both sides of the collector base junction region. Then

$$Q_{bc} = q N_{ep} (w - w_0) \quad (2.23)$$

where N_{ep} is constant epilayer concentration, w and w_0 are defined in Figure 2.2

Assuming the base is much more heavily doped than the collector so that almost the whole voltage drop occurs across the collector depletion region then w can be approximated as

$$w = \left[\frac{2\epsilon(V_{CB} + V_{BIC})}{qN_{ep}} \right]^{1/2} \quad \text{and} \quad w_0 = \left[\frac{2\epsilon V_{BIC}}{qN_{ep}} \right]^{1/2} \quad (2.24)$$

Here V_{BIC} is the collector junction built-in voltage. One can introduce a model parameter m_c (say) instead of using half power factor in (2.24) to get better approximation. Combining (2.23) and (2.24) we get the ratio

$$\frac{Q_{bc}}{Q_{bo}} = \sqrt{\frac{V_{CB} + V_{BIC}}{V_{PIF}}} - \sqrt{\frac{V_{BIC}}{V_{PIF}}} \quad (2.25)$$

as a function of V_{CB} with

$$V_{PIF} = Q_{bo}^2 / 2q\epsilon N_d \quad (2.26)$$

When V_{CB} approaches the V_{PIF} value the whole of the base region is depleted so we call this voltage the forward base

punch through voltage

The above formulation is valid so long as depletion region does not reach the heavily doped (n^+) substrate. When this happens we define the corresponding CB junction voltage as the epilayer reach through voltage. Designating it by V_{rep} we can show

$$V_{rep} = \frac{1}{2\epsilon} q N_{ep} w_{ep}^2 - V_{BIC} \quad (2.27)$$

For voltages greater than V_{rep} depletion width in the collector region practically stays at w_{ep} and junction capacitance is then almost constant. The stored charge in the space charge layer then linearly increases with V_{CB} and can be formulated by

$$Q_{bc} - Q_{ep} = \frac{\epsilon}{w_{ep}} (V_{CB} - V_{rep}) \quad (2.28)$$

$$\text{where } Q_{ep} = q N_{ep} w_{ep} \quad (2.29)$$

The ratio in this case would be (from (2.27) and (2.28))

$$\frac{Q_{bc}}{Q_{bo}} = \sqrt{\frac{V_{rep}}{V_{PIF}}} + \frac{1}{2} \frac{(V_{CB} - V_{rep})}{\sqrt{V_{rep} V_{PIF}}} \quad (2.30)$$

which simplifies to

$$\frac{Q_{bc}}{Q_{bo}} = \frac{1}{2} \left[1 + \frac{V_{CB} + V_{BIC}}{V_{PEF}} + \left(1 - \frac{V_{CB} + V_{BIC}}{V_{PEF}} \right) \sqrt{(1 - V_{PEF}/V_{PIF})} \right] \quad (2.31)$$

$$\text{where } V_{PEF} = \frac{w_{ep}}{2\epsilon} Q_{bo} \left(2 - \frac{Q_{ep}}{Q_{bo}} \right)$$

If V_{CB} approaches V_{PEF} the base region becomes fully depleted
So V_{PEF} can be called as the extrinsic forward base punch
through voltage

Under normal operation the base emitter junction is
forward biased such that $V_{BE} \approx V_{BIC}$ or $V_{CB} \gg |V_{BE} - V_{BIC}|$
Equations (2 25) and (2 31) then reforms to

$$\frac{Q_{bc}}{Q_{bo}} = \frac{\sqrt{V_{CE}}/\sqrt{V_{PIF}} - \sqrt{V_{BIC}}/\sqrt{V_{PIF}}}{1} \quad (2 33)$$

for $V_{CE} < V_{rep} + V_{BIC}$ and

$$\frac{Q_{bc}}{Q_{bo}} = \frac{1}{2} \left[1 + \frac{V_{CE}}{V_{PEF}} + \left(1 - \frac{V_{CE}}{V_{PEF}} \right) \left(1 - \frac{V_{PEF}}{V_{PIF}} \right)^{1/2} \right] \quad (2 34)$$

Thus only two parameters V_{PIF} and V_{PEF} (or V_{rep}) are sufficient to provide fairly accurate modelling of Early effect
whereas G-P requires four parameters to be evaluated

The charge Q_{be} can be considered in a simple way
Assuming one sided abrupt junction the depletion width will
be approximated by

$$x_1 = \left[\frac{2 \epsilon (V_{EB} + V_{BIE})}{q \langle NAE \rangle} \right]^{1/2} \quad (2 35)$$

where $\langle NAE \rangle$ is the average concentration of the impurities in
the base near the emitter defined by

$$\langle NAE \rangle = \frac{\int_{x_{EO}}^{x_E} N_A(x) dx}{x_E - x_{EO}} \quad (2 36)$$

Of course $\langle NAE \rangle$ shows strong depends on V_{be} However as
is clear from the Figure 2 2 this average concentration does

not vary significant in typical reverse operating mode (one can replace it by $N_A(0)$) but shows strong dependence in the forward acting mode because of the reverse grading effect close to x_{jE} . But in the forward direction the variation of V_{BE} itself is not significant so this approximation cannot in any way impair the result. So we can use an expression similar to (2.25) also for the ratio

$$Q_{be}/Q_{bo} = \sqrt{(V_{BE} + V_{BIE})/V_{PIR}} - \sqrt{V_{BIE}/V_{PIR}} \quad (2.37)$$

$$\text{where} \quad V_{PIR} = \frac{Q_{bo}^2}{2q\epsilon \langle N_A \rangle} \quad (2.37a)$$

We note from (2.37) that for $V_{BIE}/V_{PIR} \ll 1$ V_{PIR} is the base emitter voltage at which the base is fully depleted. So as before let this parameter be defined as reverse base punch through voltage.

2.3.2 Mobility Variation in the Base Region

While going from (2.6) to (2.7) the mobility within the integral in (2.6) was replaced by an average value outside the integral. In his original derivation [31] Gummel has shown that the variation of mobility gives rise to an effective widening of the base (or an equivalent increase in Gummel number) by an amount $\approx 2D_0 n_1 / v_g \approx 0.02 \mu m$. For modern days transistor this is significant and cannot be simply ignored.

The reason for this can be seen physically as follows. Because the net impurity concentration is not constant across the base region the peak of the profile occurs close to BE junction where holes have got greater mobility than those at

the falling edge of the profile close to the CB junction. Thus as majority carriers are depleted from the base as a result of an increase in V_{CE} it is the carriers with lower mobility weighting that are lost. This results in a smaller fractional decrease of effective base Gummel number and hence less pronounced dependence of I_C over V_{CE} than would be predicted from charge control approach.

The single analytical expression of mobility in a semiconductor in its simplest form can be written as

$$\mu = \frac{\mu_0}{1 + \left(\frac{N}{N_C}\right) + \frac{|E|}{E_C}} \quad (2.38)$$

where $\mu_0 = 1400 \text{ cm}^2/\text{V sec}$ is the mobility of intrinsic silicon, $\alpha = 0.72$, $N_C = 8.5 \times 10^{16}/\text{cm}^3$ and $E_C = 7.5 \times 10^3 \text{ V/cm}$ (critical field). For a standard double diffused npn transistor the net impurity concentration is given by

$$N(X) = -N_E e^{-(X/X_E)^2} + N_B e^{-(X/X_B)^2} - N_{\text{epi}} \quad (2.39)$$

where $N(X_{JE}) = N(X_{JC}) = 0$ defines the metallurgical junctions. Unfortunately the use of (2.39) does not lend itself into a simple analytical expression for our subsequent calculations. Anyway by approximating the base impurity profile by an exponentially graded profile

$$N_A(x) = \hat{N}_A e^{-\eta x/w_b} \quad (40)$$

a simple analytical solution is possible. Comparing (2.39) and (2.40) we match $N(X_{JE}) = \hat{N}_A = N_A(0)$, $N(X_{JC}) = \hat{N}_A e^{-\eta w_b}$

with w_b X_{jCO} X_{jEO} Then η is given by

$$\eta = \ln(N(X_{jEO})/N(X_{jCO})) \quad (2.41)$$

and $N(X_{jEO})$ and $N(X_{jCO})$ has to be calculated from (2.39). We also note from (2.22b) $\eta = C_F w_b$. Following a derivation somewhat similar to that of Scott and Roulston [38] we get better approximation of the ratio

$$\left[\frac{Q_{bc}}{Q_{bo}} \right] = \frac{\left(\frac{Q_C}{Q_{bo}} \right) (1 + \alpha) \left[1 - \frac{\eta V_T}{w_b E_C} + \left(\frac{Q_{bc}}{Q_{bo}} \right)^\alpha \right]}{1 + \left(\frac{Q_C}{Q_{bo}} \right)^\alpha (1 + \alpha)} \quad (2.42)$$

where $Q_C = q N_C w_b A_e / \eta$. The value of the ratio Q_{bc}/Q_{bo} to be substituted by the left hand side of (2.33) or (2.34) as the case may be. All other quantities are similarly defined. Note that the ratio Q_{bc}/Q_{bo} so obtained is less than what we have got previously without considering mobility variation. The results thus support our explanation already given at the beginning of this section.

2.3.3 Variation of τ_F and τ_R with I_C

As already mentioned the GP model is based on the modelling of total majority carrier charge in the base region. By assuming quasi-neutral condition, excess majority carrier charge has been equated with injected minority carrier charge while the latter is related with the corresponding current by charge control theory. Thus the fourth and fifth terms of (2.9) ($B\tau_F I_F$ and $\tau_R I_R$ respectively) where τ_F and τ_R has the physical significance of forward and inverse recombination life

time and B is a factor to incorporate base push out effect at high injection current) are arrived Gummel and Poon accepted them as model parameters but as we shall see shortly they indeed show significant variations with collector current as τ_f varies roughly from w_b^2/D_n to $w_b^2/4D_n$ as the system passes from low to high injection

In order to incorporate the effect of grading factor as well as variation of τ_f with I_C we can model the excess charge in terms of the excess charge density itself or by deriving an analytical expression of τ_f and τ_r as a function of corresponding current and still using charge control theory. The first method has merits in a way that it allows us to incorporate the emitter crowding effect in a straightforward manner. We will discuss here both the methods.

For its relevance we rewrite the expression (2.2a) here

$$\mu_p p j_n - \mu_n n j_p = \mu_n \mu_p kT \frac{d}{dx} (np) \quad (2.43a)$$

and then use quasi-neutrality condition $p \cong n + N_A(x)$

Einstein relation $D_n = \mu_n kT/q$ and neglect majority carrier current j_p to obtain

$$j_n = q D_n \left(\frac{2n + N_A(x)}{n + N_A(x)} \frac{dn}{dx} + \frac{n}{n + N_A} \frac{dN_A}{dx} \right) \quad (2.43)$$

This expression is quite valid in normal operation even at high injection. But in deep saturation and inverse active high injection condition the negligence towards j_p would not be a fair deal. Since the collector region Gummel number is

far less than that of the emitter region and also because of capture ratio (i.e. ratio of the capture cross section to the injected cross-section) is less than one for inverse injection the inverse active gain h_{FEI} would be much less. In spite of this fact since the current j_n results from a short base diode and j_p from a long base diode j_n remains far greater than j_p . Further owing to the low doping the epi collector region goes earlier into high injection than the relatively higher doped base region so we should expect h_{FEI} to increase with V_{CE} monotonously until high injection in the base region sets in. But the situation is much more complicated because of the presence of collector edge crowding (equivalent to emitter crowding effect for forward mode operation) the transport factor severely reduces which has an opposite effect of reducing h_{FEI} . The situation is thus complicated and to get exact analytical solution would be difficult one. Nevertheless Gummel-Poon model can be used though not rigorously.

(A) Low Injection

If everywhere $n(x) \ll N_A(x)$ equation (2.43) reduces to $j_n = qD_n \frac{1}{N_A} \frac{d}{dx} (nN_A)$. Multiplying throughout by $N_A(x)dx$ and substituting the value of $N_A(x)$ from (2.40) the above expression is integrated over the limit 0 to x . Then a little rearrangement will lead one to [27]

$$n(x) = n(0) e^{\eta x/w_b} - \frac{|j_n| w_b}{qD_n \eta} \{e^{\eta x/w_b} - 1\} \quad (2.44)$$

so with $f = e^\eta$

$$n(w_b) = fn(0) - \frac{|j_n|}{qD_n} \frac{w_b}{\eta} (f - 1) \quad (2.44a)$$

Replacing j_n by j_{cc} (2.44a) gives us

$$j_{cc} = \frac{qD_n}{w_b} \frac{\eta}{f - 1} [fn(0) - n(w_b)] \quad (2.45)$$

On multiplying both sides by A_e the emitter area and using the normalised form of carrier densities ($n_o = n(0)/N_A(0)$, $n_b = n(w_b)/N_A(0)$) this expression reduces to

$$I_{cc} = I_{fo} (n_o - \frac{1}{f} n_b) \quad (2.45a)$$

with

$$I_{fo} = \frac{qD_n}{w_b} N_A(0) \eta \frac{f}{f - 1} A_e \quad (2.46)$$

As n_o depends only on the junction voltage V_{BE} and n_b only on V_{BE} we will split the main current as $I_{cc} = I_f - I_r$ so that (2.45a) gives

$$I_f = I_{fo} n_o \quad (2.47)$$

$$I_r = \frac{1}{f} I_{fo} n_b$$

from (2.44) and (2.45) we get the following expression for excess carrier charge density

$$n(x) = n(0) e^{\frac{\eta x}{w_b}} + \frac{n(w_b) - fn(0)}{f - 1} [e^{\frac{\eta x}{w_b}} - 1] \quad (2.48)$$

This expression can be utilised to get the expression for total injected minority carrier charge $Q_{b1} = q A_e \int_0^{w_b} n(x) dx$ obviously this Q_{b1} can also be split into a forward charge Q_f

depending on n_o and thus on V_{BE} and a reverse charge depending on V_{BC} via n_b . They are

$$Q_F = Q_{bo} \frac{f(\eta - 1)f + 1}{(f - 1)^2} n_o \quad (2.49)$$

$$Q_R = Q_{bo} \frac{f(f - 1 - \eta)}{(f - 1)^2} n_b$$

Here Q_{bo} is the fixed base charge

$$Q_{bo} = q A_e \int_0^{w_b} N_A dx = q N_A w_b \frac{f - 1}{\eta f} A_e \quad (2.50)$$

(B) High Injection

Now $n(x) \gg N_A(x)$ so (2.43) simplifies to $j_n \approx 2qD_n(dn/dx)$. This equation in conjunction with (2.40) gives the simple solution for current density and carrier density

$$j_n = j_{cc} = \frac{2qD_n}{w_b} \{n(0) - n(w_b)\} \quad (2.51)$$

$$n(x) = n(0) - \{n(0) - n(w_b)\} \frac{x}{w_b} \quad (2.52)$$

In a similar way for low injection we arrive at

$$I_F = I_{fo} \frac{2}{\eta} \frac{f - 1}{f} n_o \quad (2.53)$$

$$I_R = I_{fo} \frac{2}{\eta} \frac{f - 1}{f} n_b$$

and

$$Q_F = Q_{bo} \frac{\eta}{2} \frac{f}{f - 1} n_o \quad (2.54)$$

$$Q_R = Q_{bo} \frac{\eta}{2} \frac{f}{f - 1} n_b$$

Here again the current and charge are expressed as functions of normalised carrier concentrations. To relate these densities to V_{BE} and V_{BC} respectively we use the pn product at the junctions $pn = (n + \hat{N}_A)n = n_i^2 \exp(V/V_T)$ where the neutrality condition is exploited. In normalised form we get for n_o and n_b

$$\begin{aligned} n_o(1 + n_o) &= \frac{I_s}{I_{fo}} e^{V_{BE}/V_T} \\ n_b(\frac{1}{f} + n_b) &= \frac{I_s}{I_{fo}} e^{V_{BC}/V_T} \end{aligned} \quad (2.55)$$

Here I_s is the familiar saturation current

$$I_s = \frac{f}{f-1} \frac{q D_n n_i^2}{\hat{N}_A w_b} A_e = \frac{q D_n n_i^2}{Q_{bo}} A_e^2 \quad (2.56)$$

Note that these set of equations are totally in agreement with Gummel equation. At low injection neglecting n_o , n_b in comparison with 1 or $1/f$ respectively we get from the sets (2.55) and (2.47) $I_f = I_s e^{V_{BE}/V_T}$ and $I_r = I_s e^{V_{BC}/V_T}$ the usual expressions of forward and inverse currents. And for high injection n_o , $n_b \gg 1$ and then from the sets (2.55) and (2.53) $I_f = a_{ho} \sqrt{I_s I_{fo}} e^{V_{BE}/2V_T}$ and $I_r = a_{ho} \sqrt{I_s I_{fo}} e^{V_{BC}/2V_T}$ (here $a_{ho} = \frac{2}{\eta} (f-1)/f$) same as can be obtained from Gummel equation.

Now comes the diversion from Gummel form. Gummel has defined knee current I_k as the current when minority carrier charge equals majority carrier charge or $I_k = Q_{bo}/\tau_f$ from charge control theory. Let us define I_k as the current

where the two asymptotic currents (2 47) and (2 53) intersects
Thus

$$I_k = a_{ho} \sqrt{I_s I_{fo}} e^{V_k/2V_T}$$

or

$$I_k = I_s e^{V_k/V_T} \quad (2 57)$$

where V_k is the corresponding knee voltage Eliminating V_k
from them

$$I_k = a_{ho}^2 I_{fo} = Q_{bo}/(w_b^2/4D_n) \quad (2 58)$$

Thus comparing (2 57) and (2 58) we see $\tau_f(I_k) = \frac{\tau_o^1}{2}$ where
 $\tau_o = w_b^2/2D_n$ is the simple forward transition time without
grading effect At high current τ_f is reduced by two as the
diffusion constant effectively doubles because of increase in
conductivity in the base This result is also directly
evident from (2 43) If we substitute $n(x) = N_A(x)$ there
we would get $j_n = q(2D_n) \frac{dn}{dx}$ This is the same expression as
in low injection case except that D_n is replaced by $2D_n$

From (2 47) (2 53) and (2 58) we note that at low
injection $I_f = I_{fo} n_o = a_{ho}^{-1} (I_k/a_{ho}) n_o$ and at high injection
 $I_f = I_{fo} n_o a_{ho} = (I_k/a_{ho}) n_o$ where a_{ho} is already defined or in
general $I_f = g(I_k/a_{ho}) n_o$ where $g = 1/a_{ho}$ for $n_o \ll 1$ and
 $g = 1$ for $n_o \gg 1$

We now assume that g behaves monotonically with
respect to the asymptotes of Figure 2 3 as a function of η
A fit function is proposed which satisfies all these require
ments

$$g = \frac{2 + a_{ho} + 4n_o}{(2 + a_{ho})a_{ho} + 4n_o} \quad (2.59)$$

So the general model expressions for currents and charges becomes

$$I_f = \frac{2 + a_{ho} + 4n_o}{(2 + a_{ho})a_{ho} + 4n_o} \frac{I_k}{a_{ho}} n_o - I_o$$

$$I_r = \frac{1/f + n_b}{a_{ho} + n_b} \frac{I_k}{a_{ho}} n_b - I_o \quad (2.60)$$

and

$$Q_f = Q_{bo} \frac{2 + a_{ho} + n_o}{(2 + a_{ho}) \frac{b_{lo}}{a_{ho}} + n_o} \frac{1}{a_{ho}} n_o$$

$$Q_r = Q_{bo} \frac{b_{lb}/f + n_b}{1/f a_{ho} + n_b} \frac{1}{a_{ho}} n_b \quad (2.61)$$

where $b_{lo} = \frac{(f-1)}{f(\eta-1)f+1}$ $b_{lb} = \frac{f(f-1-\eta)}{(f-1)^2}$ In (2.59) I_o is subtracted in order to make $I_f = I_o$ for $V_{BE} \ll 0$ and $I_r = -I_o$ for $V_{BC} \ll 0$

So far we have neglected the bias dependence of the fixed charge Q_{bo} and the base width w_b . If we redefine these quantities for zero bias they must be replaced by $q_1 Q_{bo}$ and $q_1 w_b$ in the previous expressions when bias is applied where $q_1 = 1 + \alpha_{be} + \alpha_{bc}$. A further consequence of these is that I_k and I_s are to be divided by the factor q_1 (see (2.58) and (2.56) respectively). These replacements incorporate base width modulation effect on the stored charges and currents and also on transit times. An approximate expression of q_1

would be $(2 - e^{-C_R |x_E|} - e^{-\eta}) / (1 - e^{-\eta})$ where C_R is defined in (2.22b). For inverse mode operation C_R has to be replaced by $C_F (= \eta/w_b)$. Also η has to be replaced by $x_C/w_b (= C_F x_C)$ wherever it arises.

Equations (2.61) and (2.62) are not real solutions but they give a realistic picture of the current and charges that obey (2.43) in the asymptotic cases. The advantage is that they enable us to derive a closed form expression for τ_f and τ_r

$$\tau_f = \int_0^{w_b} \frac{dQ_f}{I_f} \approx \frac{Q_f}{I_f} = \tau_{fo} \tau_o \quad (2.62)$$

$$\text{and } \tau_r = \int \frac{dQ_r}{I_r} \approx \frac{Q_r}{I_r} = \tau_{ro} \tau_o$$

where we have taken $\tau_o = w_b^2 / 4D_n$. Somewhat lengthy expressions are available from (2.60) to (2.62) each for τ_{fo} and τ_{ro} which reduced to $1/q^2$ at high injection and exhibit the limit $(\eta - 1 + f^{-1}) / \eta^2 q_1^2$ at low injection (where η is positive for τ_{fo} and negative for τ_{ro}).

As already mentioned at the beginning of our derivation the variation of transit time can be incorporated in two ways. If we want to stay with GP model we can reuse (2.9) as

$$q_b = \frac{Q_b}{Q_{bo}} = q_1 + B \tau_{fo} i_f + \tau_{ro} i_r \quad (2.63)$$

where we have used equation (2.58) and definition of τ_o and replaced I_f and I_r by their normalised form $i_f (= I_f/I_k)$ and $i_r (= I_r/I_k)$. Further with the help of (2.57a) equation (2.8) can be brought to the compact form

$$i_{cc} = e^{(V_{BE} - V_k)/V_T} / q_b \quad (2.64)$$

where $i_{cc} = I_{cc}/I_k$ is the normalised linking current

Note that the model parameter I_k used here through $I_k = Q_{bo}/\tau_o$ is a constant of the device structure. It can be hypothetically defined as the knee current when there is no junction space charge effect whereas the actual $I_k = Q_{bo}/(\tau_o q_1)$ is a variable quantity on account of Early effect.

The second way to attack the problem is to directly use (of course with prior modification) Q_F and Q_R from (2.61). Hence instead of (2.63) we should get

$$q_b = q_1 + \frac{2 + a_{ho} + n_o}{(2 + a_{ho}) \frac{b_{lo}}{a_{ho}} + n_o} \frac{n_o}{q_1 a_{ho}} + \frac{b_{lb}/f + n_b}{\frac{1}{f} a_{ho} + n_b} \frac{n_b}{q_1 a_{ho}} \quad (2.65)$$

where n_o and n_b are to be evaluated from (2.55)

So far at low injection we have talked about all the major effects excepting emitter crowding effect which we feel may not be so significant. We will now consider high injection effects then emitter crowding effect and conclude the chapter with a discussion on parasitics.

2.4 HIGH INJECTION EFFECTS

2.4.1 Conductivity Modulation in the Base

The onset of high injection is said to occur at a value of current at which the minority carrier current density injected into the base becomes equal to the equilibrium majority carrier density. This takes place typically for a forward bias of about 0.7 V. It should be realised that this

criterion does not represent a threshold beyond which there is an abrupt transition to high injection occurred. Rather it should be looked upon as a limit beyond which the effect of high injection phenomena on the behaviour of the transistor is significantly manifested. Actually the passage from low injection to high injection region is depicted by the smooth transition of junction voltage dependence on transported current from e^{V_{BE}/V_T} to $e^{V_{BE}/2V_T}$ in normal mode operation or e^{V_{BC}/V_T} to $e^{V_{BC}/2V_T}$ in inverse mode operation.

The high injection level effects render many of the assumptions and approximations in the low injection range invalid. But the theory developed so far is quite general and can safely be extended to this region. The only difference is that we need not require to use the rigorous expressions of α_{be} and α_{bc} and also τ_F as the formers are insignificant with respect to Q_F and the last one quickly approaches its limiting value τ_0 . But some new effects like base push out emitter and collector crowding, resistive drop in the base and collector region have to be incorporated.

2.4.2 Base Push Out Effect

Let us try to make a clear picture of this effect before going for any derivation. When the collector current is increased for a given collector base (V_{CB}) reverse bias the concentration of carriers injected from the forward biased emitter junction into the collector base space charge region is increased. These extra charges add to the space charge on the base side while they neutralise part of the

fixed immobile space charge to the collector side of the CB metallurgical junction. If the minority carrier charge density is comparable to the doped charge density, then this causes the field distribution in the collector space charge layer to change. That is the field on the base side increases while that on the collector side decreases. It is the latter effect which has the dominant influence since most of the junction voltage appears across the collector side of the space charge epi-layer. The fact that the total voltage drop across the collector-base space charge layer has to remain constant causes its collector edges to move further into the collector quasi neutral region to compensate for the reduction in field. At the same time however the increase of forward collector current results in an increase in the ohmic drop across the undepleted part of the epi-region causing a reduction of the available voltage bias across the $p-n$ junction. Consequently the depletion layer tends to shrink. One of these effects will dominate in any given situation. However it can be shown that the end result is always an effective widening of the base width when the collector current density exceeds a specific critical value for a given reverse V_{BC} . This is accompanied by an effective increase of Q_F and hence a fall in the common-emitter current gain.

Papers [7, 14, 16] dealing with base widening mechanisms generally make a distinction between the situation where the behaviour of the collector region which is next to the induced base region is ohmic (quasi saturation) and where

it is space charge controlled (carrier swamped collector region) A unified theory has been developed by Ray et al [34] which works for any bias condition We will now present a brief account of the work because of its relevance here and finally mould it according to our needs

Figure 2 4a shows the situation when base widening is present The influence of the electric field on the carrier velocity has been taken into account by the following prescription

$$v = \mu_0 E \quad \text{when } E < E_C \quad (2.66)$$

$$= \mu_0 \sqrt{E_C E} \quad \text{when } E_C < E < E_S \quad (2.67)$$

$$= \mu_0 \sqrt{E_C E_S} = v_S \quad \text{when } E \geq E_S \quad (2.68)$$

where μ_0 = low field mobility v_S = scattering limited velocity E_C & E_S are constant critical electric field For silicon $\mu_0 = 1400 \text{ cm/V sec}$ $v_S = 10^7 \text{ cm/sec}$ Referring to Figure 2 4a when the device is in quasi saturation state the collecting zone is an ohmic zone such that $j_C \approx qnv$ and

$$\frac{dE}{dx} = 0 \quad (2.69)$$

$$\text{also} \quad \int_{w_{CIB}}^{w_C} E(x) dx = V_{BC} + V_{BIC} \quad (2.70)$$

where we have neglected the voltage drop in the quasi saturation zone (which is roughly 100 ~ 200 mV) For E upto E_C ($v \leq E_C \mu_0$) n is equal to N_{ep} so that

$$j_C = q N_{ep} v \quad (2.71)$$

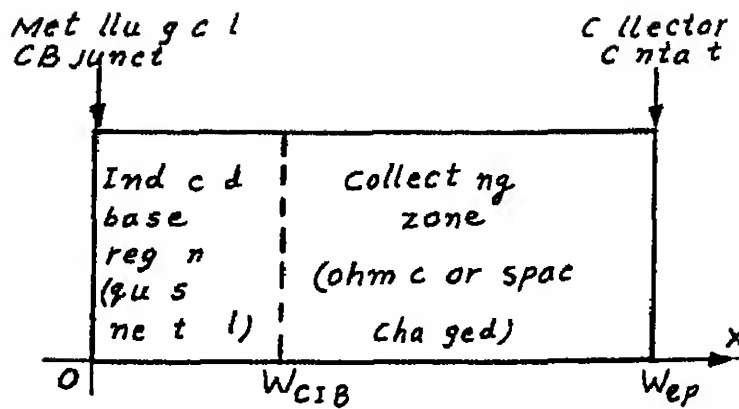


Fig 2.4(a) Location of the two zones created in the collector by the base widening effect

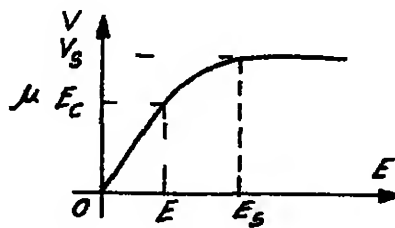
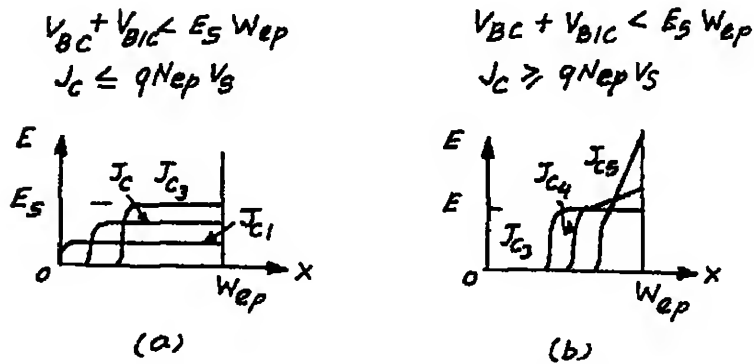


Fig 2.4(b) The carrier velocity vs the electric field



$$J < J_{c2} < J_3 \quad q N_{ep} V_s < J_{c4} < J_{c5}$$

Fig 2.5 Electric field distribution in the collector region for increasing values of the collector current in the case where $(V_{BC} + V_{BIC})$ is constant and smaller than $E_s W_{ep}$

With V_{BC} being kept constant if j_C is increased we see from (2 71) and (2 66) that the carrier velocity v and hence the electric field E in the collecting zone grows. This in turn leads to an increase of w_{CIB} in accordance with (2 70). It reaches E_S for $j_C = q N_{ep} v_S$. Beyond this limit i.e. when $j_C \geq q N_{ep} v_S$ even if all the majority carrier moves at their highest velocity this would not be sufficient to carry j_C . It is therefore necessary for extra majority carriers to be injected into the collecting zone. They are supplied by the emitter. So above this limit one should use instead of (2 71) the following

$$j_C = q(N_{ep} + n_a)v_S \quad (2 72)$$

In this condition a space charge

$$\rho(x) = \frac{q}{e} (N_{ep} - j_C/q v_S) \quad (2 73)$$

appears in the collecting zone. This manifests itself in the modification of (2 69) to

$$\frac{dE}{dx} = \frac{q}{e} (N_{ep} - j_C/q v_S) \quad (2 74)$$

Thus $E(x)$ is an increasing linear function of x . These two cases are shown in Figures 2 5(a) and (b) respectively.

The description just given above assumes implicitly that $V_{BE} + V_{BIC} < E_S w_C$

(Figures 2 6(a) and

Let us note the changes in the situation by increasing V_{BC} while keeping j_C constant. By virtue of (2 69) or (2 74) as the case may be dE/dx does not vary and the area bounded by the curve $E(x)$ versus x increases in a way dictated

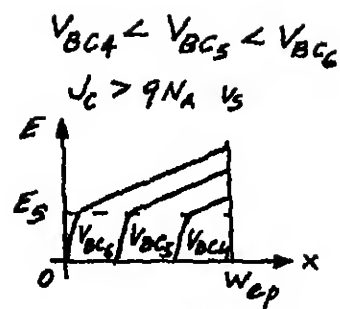
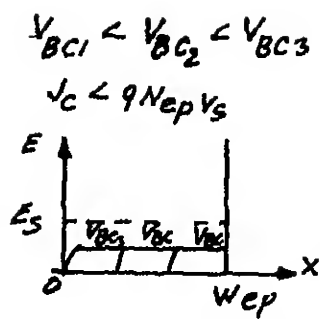


Fig 26 Electric field distribution in the collector region for increasing values of the collector bias voltage and constant value of the collector current

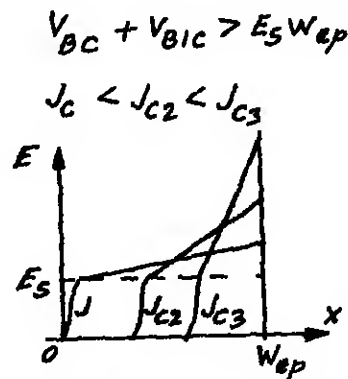


Fig 27 Electric field distribution in the collector region for increasing values of the collector current in the case where $(V_{BC} + V_{B1c})$ is constant and greater than $E_s w_{ep}$

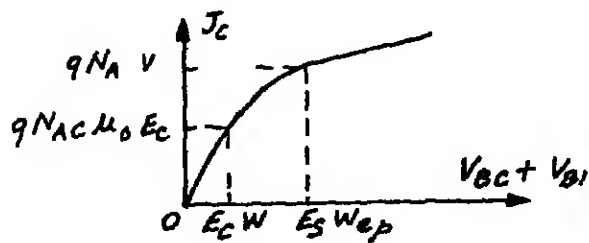


Fig 28 The critical current density J_0 as a function of $(V_{BC} + V_{B1c})$

by (2.70) Two cases must be differentiated (a) when $j_C \leq q N_{ep} v_s$ and when (b) $j_C \geq q N_{ep} v_s$ Depending on these (2.69) or (2.74) has to be used In both cases w_{CIB} increases when V_{BC} increases Here again we have assumed $V_{BC} + V_{BIC}$ remains lower than $E_s w_{ep}$

Finally the evolution of the distribution $E(x)$ for increasing j_C at constant $V_{BC} + V_{BIC} (> E_s w_{ep})$ is shown in Figure 2.7

ANALYTICAL SOLUTION So far we have seen different bias situation under which w_{CIB} occurs Let us derive an expression for it at different regions Using the appropriate set of equations from the group (2.66) to (2.74) the following relations are obtained for the current induced base width (w_{CIB})

$$(a) \quad j_C \leq q N_{ep} \mu_o E_C$$

$$w_{CIB} = w_{ep} \left(1 - \left(\frac{q \mu_o N_{ep}}{j_C} \right) \frac{V_{BIC} V_{BC}}{w_{ep}} \right) \quad (2.75)$$

$$(b) \quad q N_{ep} \mu_o E_C \leq j_C \leq q N_{ep} v_s$$

$$w_{CIB} = w_{ep} \left[1 - \left(\frac{q N_{ep} v_s}{j_C} \right)^2 \frac{V_{BIC} - V_{BC}}{E_s w_{ep}} \right] \quad (2.76)$$

$$(c) \quad j_C \geq q N_{ep} v_s$$

$$w_{CIB} = w_{ep} \left[1 - \frac{\epsilon v_s (E_s^2 / w_{ep})}{j_C - q N_{ep} v_s} \left\{ \left(1 + \frac{2(V_{BIC} V_{BC})}{\epsilon v_s E_s^2} \right) (j_C - q N_{ep} v_s)^{1/2} - 1 \right\} \right] \quad (2.77)$$

The critical current density designates the onset current for which the base widening phenomenon occurs and it is a function

of the applied voltage (see Figure 2 8)

$$(a) \quad V_{CB} + V_{BIC} \leq E_C w_{ep}$$

$$j_o = q \mu_o N_{ep} \frac{V_{CB} + V_{BIC}}{w_{ep}} \quad (2.78)$$

$$(b) \quad E_C \leq V_{CB} + V_{BIC} \leq E_S w_{ep}$$

$$j_o = q N_{ep} \mu_o \left[E_C \frac{V_{CB} + V_{BIC}}{w_{ep}} \right]^{1/2} \quad (2.79)$$

$$(c) \quad V_{CB} + V_{BIC} \geq E_S w_{ep}$$

$$j_o = q N_{ep} v_s + \frac{2 \epsilon v_s}{w_{ep}^2} (V_{CB} + V_{BIC}) - s w_{ep} \quad (2.80)$$

The base push out effect is introduced in the expression (2.64) by introducing the factor B in the fourth term where $B = \left(\frac{w_{eff}}{w_b}\right)^2 = \left(1 - \frac{w_{CIB}}{w_b}\right)^2$ (since $\tau_F \propto w_b^2$) or in the fourth term of (2.65) by $b = \left(\frac{w_{eff}}{w_b}\right) = 1 - \frac{w_{CIB}}{w_b}$ (since $Q_F \propto w_b$) and we will replace q_1 by 1

A few points can be made in this connection. The actual picture of base push out is much more complex than what is depicted here. There are many side effects which render this derivation slightly inaccurate e.g. because of edge crowding the effective collector area over which charge flows increases and this leads to an effective increase of w_b by the factor

$$\frac{w_b}{w_b} = \left[1 + \frac{w_E^2}{4w_b^2} \left(\frac{I_C}{j_o A_E} - 1 \right)^2 \right]^{1/2} \quad (2.81)$$

Secondly when $q N_{ep} V_C < j_C < q N_{ep} V_S$ the approximation of j_C by (2.71) is not justified to some extent

Thirdly in quasi saturation state the voltage drop across the induced base region is though small but comparable to that across the ohmic region for a standard $n^+p n^+$ structure. This has to be taken into account. Finally we have also neglected the zero bias depletion width when comparing w_{eff} and w_b .

2.4.3 Quasi Saturation Region in the Collector

Let us examine this region more critically. In Figure 2.9 is shown the low V_{CE} versus I_C characteristics of a typical high voltage transistor. Here for a typical base current I_{b1} the characteristics exhibits saturation from 0 to A with a resistance equal to the n^+ collector (Region I). From A to A (Region II) the slope changes and the device enters its active region at A. From A to B the collector junction is reverse biased (Region III). At the point A the equation is $V_{CEO} = R_{ep} j_{Oe} A_e$. The region A to A is called the quasi saturation region. In region I the $p-n$ junction (we denote the $epi-n$ region by n) is heavily forward biased which ensures the n region to be filled with injected holes with a concentration well in excess of the background. In addition charge neutrality requires that the electron concentration in this region be approximately equal to the excess hole concentration. Thus the region is heavily conductivity modulated and supports a negligible potential drop.

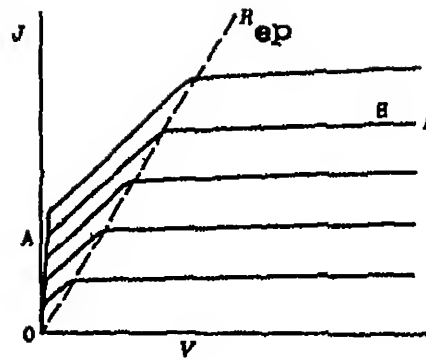


Fig 11 : Output characteristics (saturation) of power transistor

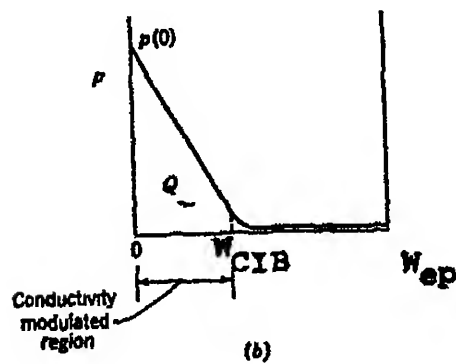
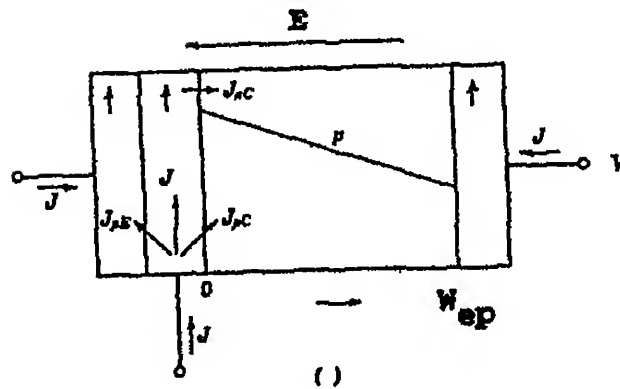


Fig 12(a) &: Carrier concentrations in the ν -region
(b)

Between A and A the ν region is conductivity modulated over a part of its length the remaining part will appear as ohmic resistance. In order to model this region it is advisable not to use second equation of the set (2.55) since V_{CB} is not easily expressible rather one should equate the pn product on either side. Defining $p_0 = p(0)/N_{ep}$ we then have

$$n_b \left(\frac{1}{f} + n_b \right) = \left(\frac{N_{ep}}{N_A} \right) p_0 (p_0 + 1) \quad (2.82)$$

In general p_0 is a complicated function of V_{CB} and I_C . Let us derive a handy expression for $p(0)$. The electron concentration in the ν -region is given by

$$n \approx p + N_{ep}$$

The electron and hole current densities are

$$j_{pc} = q \mu_p p E - q D_p \frac{dp}{dx} \quad (2.83)$$

$$j_{nc} = q \mu_n (p + N_{ep}) E + q D_n \left(\frac{dn}{dx} \right) \quad (2.84)$$

The total collector current density $j_C = -(j_{pc} + j_{nc})$ is a negative quantity for the sign convention we have used. The electric field in the collector region

$$E(x) = V_T \frac{1}{p} \frac{dp}{dx} + \frac{j_{pc}}{q \mu_p p} \quad (2.85)$$

has two components. The first one is because of forward injection of the p- ν diode the second term is because of ohmic drop across the epi-region. Since our interest is in a regime where the transistor has a significant current gain then to a good approximation we should have $j_{pc} \approx 0$ and then

$$E(x) = \frac{V_T}{p} \frac{dp}{dx} \quad \text{With } dn/dx = dp/dx \text{ we see}$$

$$j_C \approx -j_{nc} = 2q D_n \left(1 + \frac{N_{ep}}{2p}\right) \frac{dp}{dx}$$

The solution of this equation gives

$$p(x) = p(0) - \frac{j_C x}{2q D_n} + \frac{N_{ep}}{2} \ln \frac{p(0)}{p(x)} \quad (2.86)$$

If $p(x) \gg N_{ep}$ the last term of the above expansion can be omitted and $p(x)$ is thus linearly decreasing with x over that region. This is valid up to a point $x = w_{CIB}$ where

$$w_{CIB} = \frac{2q D_n p(0)}{j_C} \quad (2.87)$$

Substituting this back in (2.86) we get

$$p(w_{CIB}) = \frac{N_{ep}}{2} \ln \frac{p(0)}{p(w_{CIB})} \quad (2.88)$$

A closed form solution of this equation is not possible. However one can approximate quite reasonably $p(w_{CIB}) \approx N_{ep}$. The potential drop over this conductivity modulated region is

$$V_{CIB} = - \int_0^{w_{CIB}} E dx = - V_T \int_{p(0)}^{p(w_{CIB})} \frac{d(p(x))}{p(x)} = V_T \ln \frac{p(0)}{N_{ep}} \quad (2.89)$$

The potential drop across the unmodulated part of the ν region ($w_{CIB} \leq x \leq w_{ep}$) is Ohmic and is given by

$$V_{CZ} = \frac{j_C (w_{ep} - w_{CIB})}{q \mu_n N_{ep}} \quad (2.90)$$

$$\text{where} \quad V_{CB} = V_{CB} + V_{CIB} + V_{CZ} \quad (2.91)$$

The appropriate value of μ_n from (2 66) to (2 68) has to be substituted v_{CE} roughly the collector emitter voltage drop (v_{CE}) The termination of the quasi-saturation region for a given v_{CE} (or v_{CB}) is given by the critical current j_0 (vide equation (2 79))

The injected hole concentration $p(0)$ can be determined from charge control considerations We have seen from (2 86) the charge distribution is linear upto w_{CIB} Writing τ_{ep} as the hole life-time in the epi-region the stored charge is given by Q such that

$$\frac{Q}{A_c} = j_{pc} \tau_{ep} \cong \frac{qp(0)w_{CIB}}{2} \quad (2 92)$$

where A_c is the cross section area of the epi-region Since charge density falls linearly with distance in the quasi-saturation region one can write

$$\frac{dp}{dx} \cong - \frac{p(0)}{w_{CIB}} = - \frac{j_c}{2qD_n} \quad (2 93)$$

so that from (2 92) and (2 93)

$$p(0) = 2 \left(\frac{j_c j_{pc} \tau_{ep}}{q^2 D_n} \right)^{1/2} \quad (2 94)$$

and

$$w_{CIB} = 2 \left(\frac{j_{pc} \tau_{ep} D_n}{j_c} \right)^{1/2} \quad (2 95)$$

where modulation of the p-base region has been ignored here

The onset of quasi saturation occurs at A Writing this current density by j_T and substituting $x = w_{ep}$

$$j_T = \frac{2q D_n p(0)}{w_{ep}} \quad (2.96)$$

The study of quasi saturation is important for a device acting as a switch since it increases the turn on time and hence power dissipation also

2.5 EMITTER REGION SOLUTION [29-38]

The doping of the emitter region is such that the semiconductor is degenerate. So far we have ignored this factor which is O.K. for low level operations. A closed form solution taking the variation of doping level, emitter degeneracy, band gap narrowing, high level of injection etc. into account is too much involved. Roulston et al. has derived the following rigorous expressions

$$n(x_b) = \frac{(N_E(x_e) - N_A(x_e))e^{V_{BEJ}/V_T} + N_A(x_b) - N_E(x_b)}{(e^{2V_{BEJ}/V_T} - 1)} \quad (2.97)$$

$$p(x_e) = \frac{-(N_E(x_b) - N_A(x_b))e^{V_{BEJ}/V_T} + N_E(x_e) - N_A(x_e)}{(e^{2V_{BEJ}/V_T} - 1)} \quad (2.98)$$

where $n(x_b)$, $p(x_e)$ denotes the minority carrier charge densities at the base and emitter side of the junction depletion region. V_{BEJ} is the net potential across the junction and

$$V_{BEJ} = V_{BIE} - V_{BE}$$

2.6 EDGE CROWDING EFFECT

The analysis of the transistor is mainly based on the one dimensional current flow assumption. However, in any practical transistor, there will be a crossflow of base current towards the base terminal. This flow of base current parallel to the emitter-base junction will cause a transverse voltage drop which makes less of the applied base-emitter voltage to appear at the centre of the junction as against the edge (see Figure 2.11). This increases injection of minority carriers from the edge of the emitter as compared to that at the centre, thus causing the current to crowd around the periphery of the emitter (close to the base metal contact). Emitter edge crowding becomes significant when the difference in voltage between the centre and edge of the base is of the order of thermal voltage. While studying low injection operation, the above phenomenon may be ignored as the base current itself (and hence the lateral voltage drop) is small. However, the current crowding at the base region underneath the edge of the emitter causes earlier onset of the conductivity modulation and other high injection phenomena there. The most serious concern with this effect is that it reduces the power rating of the transistor. For compact modelling, it must be taken into account though that leads to unavoidable complication.

Several papers [12, 16, 23, 25] are listed at the end which deal with this effect. Owing to the inherent complexity of this problem, mixed with other effects, everyone has to make some ridiculous () assumptions to get closed form

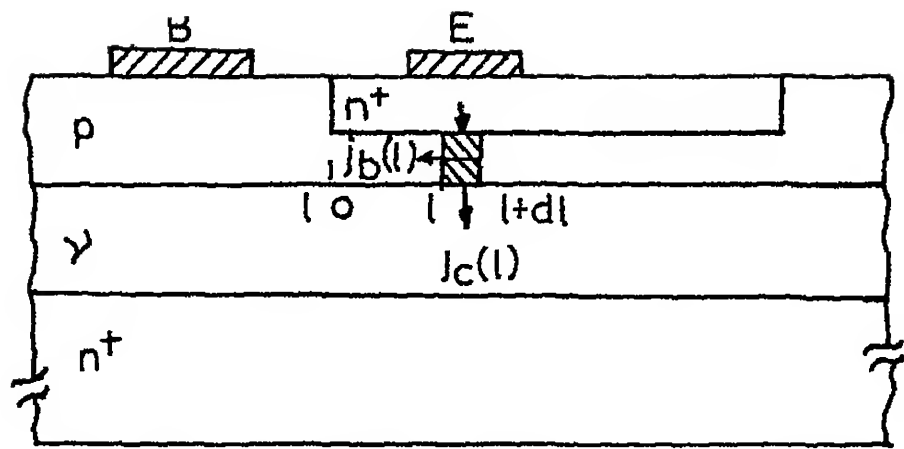


Fig 211

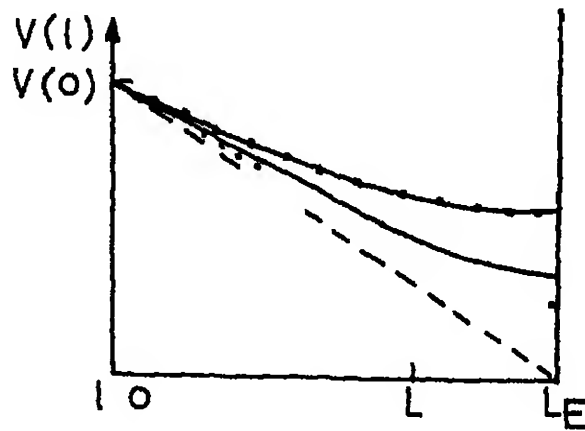


Fig 212a

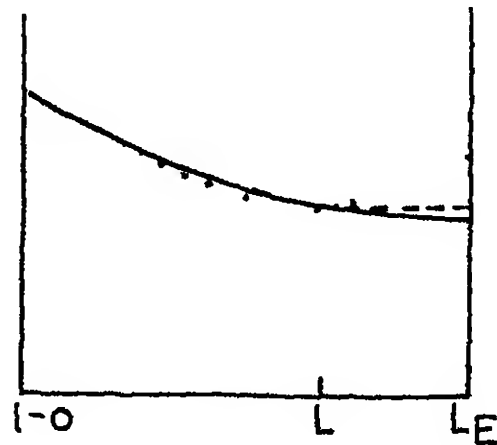


Fig 212b

Fig 211 Typical cross section of a transistor with transverse axis l chosen

Fig 212(a) Showing the voltage drop occurs across the base under different approximations
(b) Comparison between actual voltage profile & that postulated by (200)

analytical solutions We strongly feel that these does not give true picture of the situation over most part of the operating region As for example the paper [23] by J R Hauser seems to be most reasonable amongst them But it starts with the assumptions amongst which (a) the ignorance of conductivity modulation in the base whereby R_b is made constant and i_{cc} goes as $i_s e^{V(x)/V_T}$ (low injection limit) (b) is a constant are most seriously objectionable especially in high injection regime where this very effect is important

We propose to give some new model under most reasonable assumptions They are

- 1 The emitter region represents an equipotential plane
- 2 The vertical plane perpendicular to l axis at $l = 0$ the edge of the emitter contact is at equipotential
- 3 R_b is not a function of voltage (this may be omitted)
- 4 We start with single base stripe (I type) metal contact though the theory can easily be extended for double stripe contacts

Let us start with seeking how the potential profile changes as one passes from edge to the centre in the base region Throughout our discussions we shall assume the resistance R_b from the base metal contact to the section ($l = 0$) in the base is a constant quantity If we can replace the part of the base region beneath the emitter region by a lumped resistance r_b and further assume the whole of the base hole current traverses this distance (L_E) being originated from the centre of the junction (point injection) then voltage

would have fallen linearly (for npn transistor) from edge to the centre with a gradient $\frac{dV(l)}{dl} = -\frac{r_b I_b}{L_E}$ so that $V(l) = -r_b I_b (l/L_E)$ (see dashed line - - in Figure 2 12a) Because of distributive effect the gradient (magnitude) itself rather linearly decreasing and finally becomes zero at $l = L_E$ We then would have $V(l) = -r_b I_b [(l/L_E) - \frac{1}{2}(l/L_E)^2]$ (see dotted line in Figure 2 12a) where we have assumed the base current density $j_b(l)$ is uniform all over the base region But this is not the case as the voltage at the edge ($l = 0$) is higher than that at the centre ($l = L_E$) and current density has exponential dependence on the base emitter voltage (the emitter surface is equipotential region) Hence larger portion of I_b is originated from the edges than the centre This fact brings about a third order term $(l/L)^3$ in the expansion of $V(l)$ (continuous line — in Figure 2 12a) and so on The conductivity modulation in the base complicates the situation in that case the coefficients of $(l/L)^1$ in the expansion of $V(l)$ suffer change For high base currents the base profile shows sharper fall upto L followed by a slow fall which ends at L_E (shown by continuous line in Figure 2 12b) In that case expanding $V(l)$ in the power series of l/L_E would not be justified We propose to use a scheme whereby $V(l)$ has to be modelled by a series expansion of (l/L) upto L (dotted line in Figure 2 12b) and then by a constant value (dashed line in Figure 2 12b) from L to L_E The point L would be determined by the fact that the positive and negative error (shown by hatched region) comes equal

We now introduce the following dimensionless variables $x = l/L$ $l_r = L/L_E$ and the normalised voltage drop $v(x) = v(l) = v(l)/V_T$ in the base According to the above scheme we postulate

$$\begin{aligned} v(x) &= \sum_{n=1}^{\infty} C_n x^n \quad \text{for } 0 \leq x \leq 1 \\ &= \sum C_n v(1) \quad \text{for } 1 \leq x \leq 1/l_r \end{aligned} \quad (2.99)$$

where C_n s are parameters (function of l_r) to be determined Normally upto third or fourth term is retained in the expansion of (2.99) which ensures sufficient accuracy For latter convenience we put down here the following expansions

$$e^{v(x)} = \sum_{n=0}^{\infty} (n+1) k_n x^n \quad \text{for } 0 \leq x \leq 1 \quad (2.100)$$

$$e^{v(x)/\eta_e} = \sum_{n=0}^{\infty} (n+1) k_{en} x^n$$

where k_n is another set of parameters From (2.99) and (2.100) one can establish the following identities

$$\begin{aligned} k_1 &= \frac{1}{2} C_1, \quad k_2 = \frac{1}{3} (C_2 + C_1^2/2), \quad k_3 = \frac{1}{4} (C_3 + C_1 C_2 + C_1^3/6) \\ k_4 &= \frac{1}{5} (C_4 + C_2^2/2 + C_1 C_3 + C_1^2 C_2/2) \quad \text{and so on} \end{aligned} \quad (2.101)$$

The parameters k_{en} can be obtained likewise by replacing C_n by C_n/η_e in the identities of (2.101) We further use the following notations r_b the sheet resistivity in the base region defined as the resistance of the slab of cross sectional area $w_b H_E$ (where H_E is the breadth of the emitter junction)

and length unity Using (2 40) and (2 50) we see its value given by

$$r_{bo} = 1/(\mu_p Q_{bo}/L_E) \quad (2 102)$$

where r_{bo} is the same as r_b when no bias is applied Hence

$$r_b(x) = 1/(\mu_p Q_b(x)/L_E) = \frac{r_{bo}}{q_b(x)} \quad (2 102a)$$

(In absence of conductivity modulation $r_b \approx r_{bo}/q_1$)

At the emitter edge in the base ($x = 0$) we have

$r_b(0) = \frac{r_{bo}}{q_b(0)}$ From intuition we can at once get the value of C_1 as

$$C_1 = \left. \frac{dv(x)}{dx} \right|_{x=0} = \frac{L}{V_T} \left. \frac{dv(1)}{dl} \right|_{l=0} = \frac{r_b(0) I_b}{V_T} l_r \quad (2 103)$$

Let us divide the junction surface area into a large number of stripes of length H_E and thickness dx The base current density $j_b(1)$ would be uniform over any typical stripe and varies monotonously from stripe to stripe in view of (2 99) The current originated from a typical one would be $j_b(1) H_E dl$ and the total current $I_b = \int_{l=0}^{L_E} j_b(1) H_E dl$ Transforming the integration variable from l to x along with the help of (2 13) we can write

$$I_b = l_r I_1 e^{v_{be}(0)} \int_0^1 e^{v(x)} dx + I_2 e^{v_{be}(0)} \int_0^1 e^{v(x)/\eta_e} dx \quad (2 104)$$

where $v_{be}(0) = V_{BE}(0)/V_T$ This on inserting the expression for $e^{v(x)}$ from (2 100) transforms to the following identity

$$1 = 1_r \left[i_{10} \sum_{n=0}^{\infty} k_n + i_{20} \sum_{n=0}^{\infty} k_{en} \right] \quad (2.104a)$$

$$\text{where } i_{10} = \frac{I_1}{I_b} e^{v_{be}(0)} \quad i_{20} = \frac{I_2}{I_b} e^{v_{be}(0)/r_e} \quad (2.104b)$$

One can take the integration upper limit in (2.104) to $1/1_r$ also

(A) Low injection case

The voltage drop at a distance l from the edge in the base

$$v(l) = - \int_0^l dr_b(l) \left[I_b \int_0^l j_b(l) H_E dl \right]$$

with $dr_b(l) = r_b dl$ (ignoring conductivity modulation) and transforming the variable index from l to x

$$\begin{aligned} v(x) &= - \frac{r_b I_r}{V_T} \int_0^x dx \left[I_b - A_e I_r \int_0^x j_b(x) dx \right] \\ &= - \frac{r_b I_b}{V_T} I_r \int_0^x dx \left[1 - I_r (i_{10} \sum_{n=1}^{\infty} k_{n-1} x^n \right. \\ &\quad \left. + i_{20} \sum_{n=1}^{\infty} k_{en-1} x^n) \right] \\ &= C_1 x - C_1 I_r \left[i_{10} \sum_{n=2}^{\infty} k_{n-2} x^n / n - i_{20} \sum_{n=2}^{\infty} k_{en-2} x^n / n \right] \end{aligned} \quad (2.105)$$

Note that we have debarred from giving upper limit to the summations. It is an option to the user to specify it and normally 4 or 5 is sufficient. Comparing (2.99) with (2.105) we see for $n = 2$ to ∞

$$C_n = - I_r C_1 (i_{10} k_{n-2} + i_{20} k_{en-2}) / n \quad (2.106)$$

where C_1 is given by (2 103)

The expression^{for} collector current density in normalised form (from (2 63) and (2 64)) would be

$$i_C(x) \approx i_s \frac{e^{V_{BE}(x)/V_T}}{q_b(x)} - i_C(0) e^{v(x)} \left[\frac{q_b(x)}{q_b(0)} \right]^{-1} \quad (2 107)$$

Now $q_b(x) = q_1 + q_2(x) = q_1 + B\tau_{fo} i_C(x)$ and $q_b(0) = q_1 + q_2(0) = q_1 + B\tau_{fo} i_C(0)$ Defining $q_{2r} = q_2(0)/q_b(0)$ it can be shown (2 107) to be approximated by

$$i_C(x) \approx i_C(0) e^{v(x)} [1 + q_{2r}(1 - e^{v(x)}) + q_{2r}^2(1 - e^{v(x)})^2] \quad (2 108)$$

The corresponding expression for the linking current (taking upto second term in (2 108))

$$i_{cc} = i_r i_C(0) \left[\sum_{n=1}^{\infty} k_{n-1} + q_{2o} \sum_{n=1}^{\infty} k_{n-1} (1 - n \sum_{n=0}^{\infty} \frac{n+1}{n+n^2} k_n) + \frac{q_{bo}}{q_{bL}} (1/i_r - 1) e^{v(1)} \right] \quad (2 109)$$

If we take into account the modulation of base resistivity then $r_b(x) = r_b(0) [q_b(x)/q_b(0)]^{-1}$ where the bracketted quantity is already evaluated while passing from (2 107) to (2 108) Equation (2 108) is modified to

$$v(x) = C_1 x - q_{2r} \sum_{n=2}^{\infty} k_{n-2} x^n - C_1 i_r i_{10} \left[\sum_{n=2}^{\infty} k_{n-2} x^n / n - q_{2r} \sum_{n=2}^{\infty} \sum_{n=1}^{\infty} k_{n-2} k_n \frac{n+1}{n+n^2} x^{n+n} \right] \quad (2 110)$$

where we have neglected the recombination-generation current component of I_b as it is insignificant in this and high injection region. Correspondingly (2 106) modifies to (for $n \geq 2$)

$$C_n = -C_1 l_r l_o k_{n-2} \left[\frac{1}{n} + \frac{q_2 r}{l_r l_o} - \frac{q_2 r}{n} \sum_{n=1}^{n-1} (n+1) k_{n-n-1} k_n \right] \quad (2 111)$$

and C_1 would be given by (2 103). The sequence for evaluation of these parameters are as follows. We take $l_r = i_{cc}/i_c(0)$ and then find out the parameters (with the help of (2 101), (2 103) and (2 111)) according to the chain $l_r \rightarrow C_1 \rightarrow k_1 \rightarrow C_2 \rightarrow k_2$ upto the number that depends on the user. Then use these k_n s in (2 109) and solve it by Newton-Raphson technique to get l_r . The parameters finally can be redetermined by using this l_r . Only one iteration is sufficient as the final result does not depend critically on l_r .

The dc or low frequency base resistance can be calculated from considering the power dissipated by the base current. Hence we define effective base resistance by

$$R_b = \frac{1}{I_b^2} \int_0^L dr_b(1) \left[I_b - \int_0^1 j_b(1) H_E dl \right]^2$$

or

$$R_b = l_r r_{bo} \int_0^1 \frac{R_{bo}}{R_b(x)} dx \left[1 - l_r l_o \sum_{n=1}^{\infty} k_{n-1} x^n \right]^2 \quad (2 112)$$

At low injection with no conductivity modulation the ratio $r_{bo}/r_b(x)$ can be taken as unity. In that case (2 112) is worked out to be

$$R_b = \frac{1}{r} r_{bo} \left[1 - 2 \frac{1}{r} \frac{1}{r_{bo}} \sum_{n=2}^{\infty} \frac{k_{n-2}}{n} + \frac{1}{r} \frac{1}{r_{bo}} \sum_{n=2}^{\infty} \sum_{n=1}^{n-1} \frac{k_{n-n-1} k_{n-1}}{n+1} \right] \quad (2.113)$$

where $R_{b_{\text{line}}}$ designates the said resistance for low injection no conductivity modulation. If one would like to incorporate the latter effect then appropriate expression for the ratio $q_{bo}/q_b(x)$ has to be inserted as have already been done in (2.108). With this modification (2.112) is again solved for we here put down only the final result

$$R_{b_{\text{line}}} = R_{b_{\text{line}}} + \frac{1}{r} r_{bo} \frac{1}{r_{bo}} q_{2r} \left[2 \sum_{n=2}^{\infty} \sum_{n=0}^{\infty} \frac{k_n}{n} \frac{n-1}{n} - \frac{1}{r} \frac{1}{r_{bo}} \sum_{n=2}^{\infty} \sum_{n=0}^{n-1} \sum_{n=1}^{n-n} \frac{k_{n-n-1} k_n}{n} \frac{n+1}{n} \right] \quad (2.114)$$

where $R_{b_{\text{line}}}$ is the base resistance and low injection with conductivity modulation. Physical interpretation can be given for the occurrence of the various terms in (2.113) and (2.114). We see for extreme low injection whence $\frac{1}{r} \approx 1$, $k_0 = 1$ and all other $k_n \rightarrow 0$ both the expressions reduce to $r_b/3$.

(B) High injection case

The approximation that holds in this region is $q_1 < q_2(x)$. One can then perform the same series of calculations as has been done in low injection case. We will put down only the salient steps here.

The normalised collector current density $i_c(x)$ is given by (2 107) We reformulate it as

$$i_c(x) = \frac{i_c(0) q_{bo} e^{v(x)}}{B \tau_{fo} i_c(x)} \left[1 + \frac{q_1}{B \tau_{fo} i_c(x)} \right]^{-1}$$

$$\text{or } i_c(x) \cong i_o e^{v(x)/2} \left[1 + \frac{q_1}{q_{2o}} e^{v(x)/2} \right]^{-1/2} \quad (2 115)$$

$$\text{where } i_o = \left(\frac{i_c(0) q_{bo}}{B \tau_{fo}} \right)^{1/2} \text{ and } q_{2o} = B \tau_{fo} i_o \quad (2 115a)$$

Defining $q_h = \frac{1}{2} \left(\frac{q_1}{q_{2o}} \right)$ eqn (2 115) in expanded form (upto second order) appears as

$$i_c(x) \cong i_o \left[e^{v(x)/2} - q_h + \frac{1}{2} q_h^2 e^{-v(x)/2} \right] \quad (2 116)$$

with

$$i_c(0) = i_o \left(1 - q_h + \frac{1}{2} q_h^2 \right) \quad (2 116a)$$

The base resistance as a function of x is given by

$$\begin{aligned} r_b(x) &= \frac{r_{bo}}{q_b(x)} \\ &= \frac{r_{bo}}{q_{2o}} \left(e^{-v(x)/2} - q_h e^{-v(x)} + \frac{1}{2} q_h^2 e^{-\frac{3}{2}v(x)} \right) \end{aligned} \quad (2 117)$$

Using (2 115a) and (2 116a) in (2 117) at $x = 0$

we get

$$r_b(0) = \frac{r_{bo}}{q_b(0)} \quad (2 117a)$$

The expression for $v(x)$ is derived with the help of (2 117) and the resulting expression is compared with (2 99). This at once gives an expression of C_n similar to that (2 106) in low injection case

$$C_n = C_1 \left(\frac{i_c(0)}{i_o} \right) [k_{1/2, n-1} - \alpha_h k_{1, n-1} - \frac{1}{l_o} l_r \{ \sum_{n=2}^{n-2} \frac{k_{n-n-2} k_{1/2, n}}{n} - \alpha_h \sum_{n=0}^{n-2} \frac{n+1}{n} k_{n-n-2} k_{-1, n} \}] \quad (2 118)$$

where C_1 is as in (2 103). The coefficients $k_{\eta, n}$ (where η can be $1/2, -1$ etc.) has to be evaluated from (2 101) in the same way excepting that C_n has to be replaced by C_n/η .

The corresponding expression for collector current density

$$i_{cc} = \frac{1}{l_r} \int_0^{l_r} i_c(x) dx$$

on using (2 116) we finally get

$$i_{cc} = \frac{1}{l_r} i_o \left[\sum_{n=1} k_{-1/2, n-1} - \alpha_h + \frac{1}{2} \alpha_h^2 \sum_{n=1} k_{1/2, n-1} + \left(\frac{1}{l_r} - 1 \right) e^{v(1)/2} (1 + 2\alpha_h e^{v(1)/2})^{-1/2} \right] \quad (2 119)$$

The effective resistance at high injection

$$R_{bh} = r_{bh}(0) \sum_{n=2} [k_{-1/2, n-2} - \alpha_h k_{-1, n-2} - \frac{1}{l_r} l_o \{ \sum_{n=0}^{n-2} \frac{n+1}{n} (k_{-1/2, n} - \alpha_h k_{-1, n}) k_{n-n-2} \}] \quad (2 120)$$

where $r_{bh}(0) = \frac{r_b(0)l_r}{q_{20}}$ At extreme high injection

$$R_{bh} \cong r_{bh}(0) \left[1 - q_n - \frac{1}{2} l_r l_{10} (1 - q_n) \right] \quad (2.120a)$$

Thus at extreme high injection the base resistance falls inversely with the collector current

So far we have developed the situation for single base stripe contact. For double stripe contact the theory can be easily extended. In this case L_E = half of the emitter length. I_b , I_c appeared in the previous expressions should be considered as half of the terminal currents. At high injection the theory developed remains essentially the same. At low injection one should include a factor $(1 - \frac{1}{2} l_r x)$ to $dr_b(1)$ or $dr_b(x)$ wherever it arises.

The sheet charge density of excess carrier (q_{bf}) also appears to be modulated by the edge crowding effect. The expression for q_{bf} and n_0 is given in (2.65) and (2.55) respectively where n_0 is a function of x because of y -crowding effect. Defining

$$N_0 = n_0(0)(1 + n_0(0)) \quad (2.121)$$

where the first suffix with $n_0(0)$ represents it is at the emitter surface and the zero in the bracket defines the quantity at $x = 0$ or $1 = 0$ we at once get from (2.55) and (2.121)

$$n_0(1 + n_0) = N_0 e^{V(x)} \quad (2.121a)$$

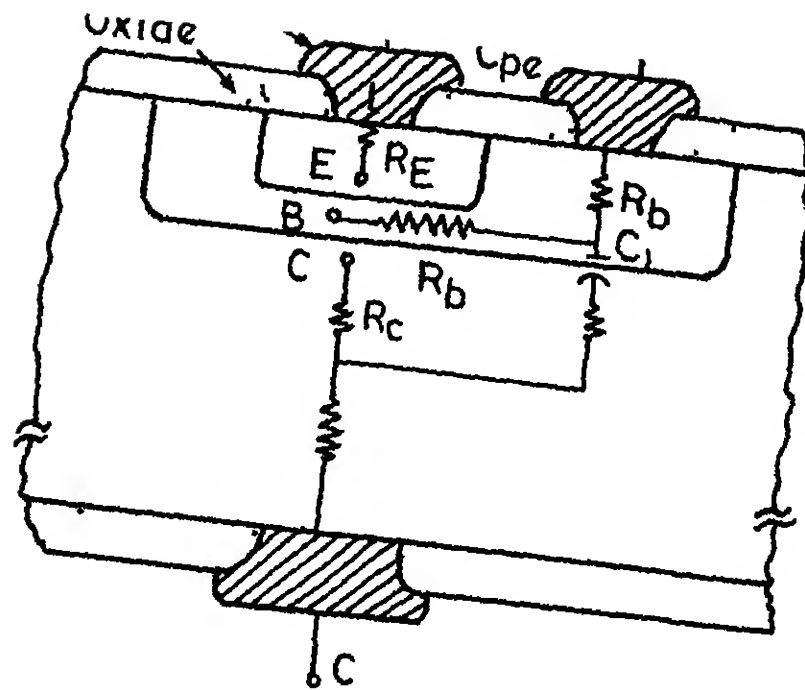
Then

$$\begin{aligned}
 q_{bf} &= l_r \int_0^{1/l_r} q_{bf}(x) dx \\
 &= l_r \left[\int_0^1 q_{bf}(x) dx + (1/l_r - 1) q_{bf}(1) \right] \quad (2.122)
 \end{aligned}$$

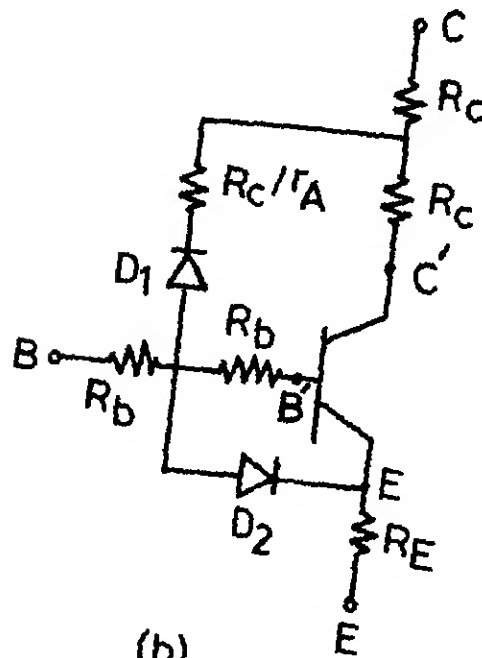
This integration can best be evaluated by numerical techniques using Legendre-Gauss quadrature rule. The integration limit is changed from (0 to 1) to (-1 to +1) by introducing the variable ξ so that $x = \xi/2 + 1/2$. First $n_0(x)$ has to be evaluated from (2.121a) for a particular x and then to be used in (2.65) to find out $q_{bf}(x)$. This is then inserted in (2.122) and the integration is carried out as summation.

2.7 PARASITIC EFFECTS

Schematic cross section of a typical transistor and its parasitic effects modelled by equivalent lumped elements are depicted in Figure 2.13(a) and (b) respectively. At high frequency the equivalent circuit is much more complicated as the reactance because of lead inductances also start becoming significant. The diode D_2 is there to represent the lateral injection from emitter to base through the side walls of the emitter. This is a long base diode. Similarly D_1 models the diode action through the inactive part of the collector region which is important when the latter itself is acting as emitter in inverse active mode. This is also a long base diode. The capacitance C_{pe} is the capacitance between the emitter and base metal contacts and C_i is the capacitance of the inactive part of the base region. One can assume



(a)



(b)

Fig 213(a) Schematic cross section of a transistor with parasitic elements over lay on it
(b) Intrinsic part of the transistor and lumped equivalent circuit of the parasitic elements

$$C_i = C_i(V_i) = r_A C_C(V_i) \quad (2.123)$$

where r_A is the ratio of the active to inactive part of the base region. Roughly

$$r_A = 1 - A_C/A_E \quad (2.123a)$$

and the voltage V_i is given by

$$V_i = V_{bc} + (r_b/q_b)I_b - R_C I_C \quad (2.124)$$

The modelling of D_i comes automatically in I_{be1} and I_{be3}

In inverse active mode GP model miserably fails. This is because the basic assumptions behind the derivation of model are violated. GP model remains valid when α is close to 1. But in inverse active mode α differs much from unity. Since the collector doping level is much less than that of base or the ratio $G_C/G_B \approx h_{FEI}$ is not large. The collector (acting as emitter) injection efficiency is small. Secondly because collector to emitter area ratio is less than 1, the transport factor is also considerably less than 1.

In order to stick with GP model we once again start with the basic equation (2.2a) and divide throughout by $p\mu_p j_n$ to get

$$j_n \left(1 - \frac{n\mu_n j_p}{p\mu_p j_n}\right) = \mu_n kT \frac{d}{dx} (np) \quad (2.125)$$

and apply it over the intrinsic symmetrical transistor (shown by dotted extension in Figure 2.13a). We cannot neglect the hole current j_p this time and write $j_p/j_n = G_B/G_C = g_{be}(\alpha_{FEI})$. Using quasi neutrality condition $p = n + N_A$

we reform the above equation to

$$j_n \left(1 - \frac{n}{n + N_A} \mu_r g_{bc} \right) = \frac{q D_n}{p} \frac{d}{dx} (np) \quad (2.125a)$$

where $\mu_r = \mu_n / \mu_p$. At low injection $n \ll N_A$ at any point in the base. Integrating the above expression from collector to emitter assuming transport factor to be unity we arrive at

$$j_n \left(\int_{x_C}^{x_E} \frac{p}{D_n} dx - \mu_r g_{bc} \int_{x_C}^{x_E} \frac{ndx}{D_n} \right) = q [np]_{x_C}^{x_E} \quad (2.125b)$$

Multiplying by $A_e q$ all throughout and assuming D_n to be constant

$$j_n (Q_b - \mu_r g_{bc} Q_{br}) = A_e q^2 (n_E p_E - n_C p_C) \quad (2.125c)$$

We finally get

$$j_n = \frac{q^2 D_n A_e n_1^2 (1 - e^{V_{BC}/V_T})}{Q_{bo} (q_1 + (1 - \mu_r g_{bc}) q_{br})} \quad (2.126)$$

or

$$I_n = - \frac{I_s (e^{V_{BC}/V_T} - 1)}{q_1 + (1 - \mu_r g_{bc}) q_{br}} \quad (2.126a)$$

where I_s is given by (2.8) and

$$g_{bc} = \frac{\frac{\eta D_n}{w_b N_A} \frac{1}{1 - f^{-1}}}{\frac{D_p}{N_{ep} L_p} \coth \frac{w_{ep}}{L_p}} \quad (2.127)$$

This is the expression for transported current in inverse active operation. Since the collector region enters rather earlier in the high injection region than in the base this

$$\beta_R = \frac{\eta D_n / (w_b \hat{N}_A)}{(1 - f^{-1}) \left(\frac{D_p}{N_{ep} L_p} \coth \frac{w_{ep}}{L_p} + r_A J_s / q \right)} \quad (2.132)$$

We thus see the gain in inverse active is much smaller because of low doping to the collector site ($N_{ep} \ll \hat{N}_A$) and because of the presence of the overlap diode D_1 (manifested via J_s)

2.8 SUMMARY

So far we take the pain to study in great detail about all the known major events that occurs in various modes of operation of a transistor. It is not viable to incorporate all of them in a single package and extract the relevant parameters with acceptable accuracy. Anyway one can cleverly pick up data from certain regions where some or the other effects are predominant and hence the relevant parameters may be extracted which can be subsequently used for modelling other regions. One may have to reiterate among the various stages until an universal convergence is reached. In our discussion we have indicated different approaches for modelling a particular effect. However we will choose the one which suits well within GP model. In Chapter IV we will first consider some of the numerical techniques and then we will make a systematic approach to extract the model parameters.

CHAPTER 3

TRANSISTOR CURVE TRACER

3.1 INTRODUCTION

The modelling of higher order effects (e.g. variation of base resistance with collector current) requires accurate measurements and special set-ups. Accordingly a special purpose curve tracer has been designed. It operates at frequencies around 1 kHz so that both transistor noise as well as power line interference can be averted. The system is insensitive to the scanning input waveform. Moreover it can be used for measurements on JFETs, MOSFETs, UJT etc. in addition to BJTs.

3.2 BASIC BUILDING BLOCK

The basic concept behind the system is formulated in the block diagram as shown in Figure 3.1. The basic idea is simple. The input ac signal is converted to an ideal rectified output excepting for a possible multiplication factor. It is then applied to the collector point via a small sampling resistance R_s and collector series resistance R_c if any. The same input signal is sensed by a ZCD (zero crossing detector) or a peak detector (both positive and negative) which gives digital output levels. This is subsequently fed to a frequency multiplier (so that for any collector sweep a new base step is generated). The output signal is used as clock of an up/down counter. The digital outputs of the counter are fed to a DAC followed by :

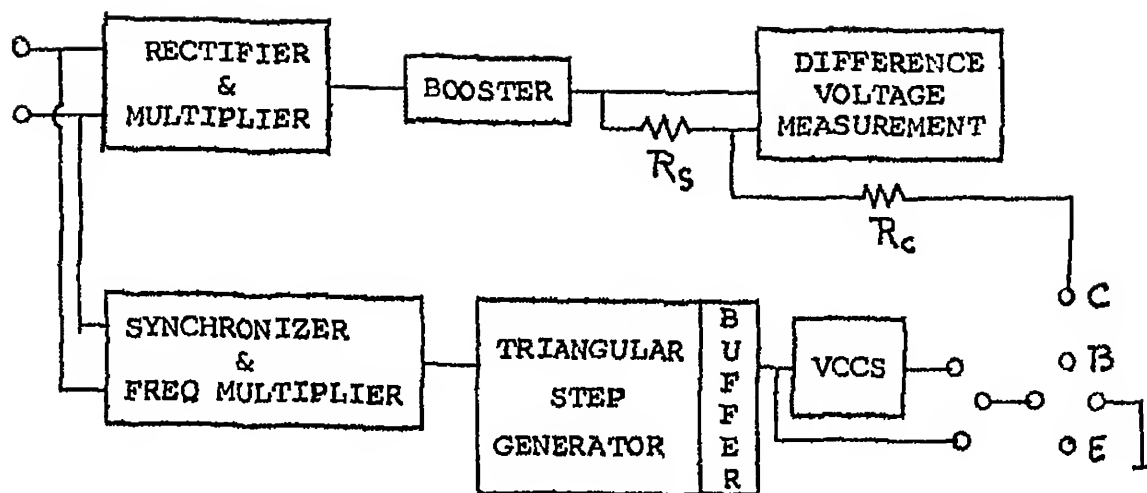


Fig 3 1a Block diagram of the curve tracer

multiplying DAC (rather acting as an attenuator) so as to generate saw tooth/triangular wave as the case may be. This output is then processed successively through a buffer and then a linear VCCS. The output of the buffer (V) as voltage step or the output of the VCCS as current step can be applied to the input terminal (T). It is then connected to the base (B) or emitter (E) while the other to the ground by using the ganged switch depending on whether we are interested in CE configuration or CB configuration. If the signals from appropriate points are picked up (e.g. in order to plot output characteristics i.e. I_c - V_{ce} family of curves with I_b as parameter, the C point is connected to X-channel and Y point to Y channel while keeping oscilloscope in XY mode) a steady picture would be available. This is then stored for subsequent use or for getting a hard copy.

3 3 1 Collector Sweep Circuit

The system indicated in Figure 3 3 gives full wave rectification with/without inversion and with a gain R/R_1 controllable by one resistor R_1 followed by a current booster circuitry. This has the advantage over ordinary rectifier that it does not suffer from zero crossing distortion. If a sinusoidal voltage whose peak value is less than the cut-in voltage V (0.6 V) of a diode is applied to an ordinary rectifier circuit we get output to be zero for all the times. And for a low level signal there is appreciable phase lag in zero crossing. By placing the diodes in the feedback loop of an OPAMP the cut in voltage is divided by the open loop gain A_V of the amplifier ($V_{Y_{eff}} = V_Y / |A_V| \approx 60 \mu V$ for $A_V = 10^5$) and the diode acts like an ideal rectifier. Though a straightforward modification of the ordinary rectifier (whereby each diode is replaced by an ideal diode so described and a summer is introduced at the end) is feasible but the choice of our circuit is obvious as in the former case each input OPAMP is strained by large differential voltage across its inputs and also it requires an extra stage a summer at the output. Moreover the gain is easily controllable in our adopted system by only varying the resistance R_1 .

The basic operation of the circuit is as follows. Let us consider first the half cycle where v_{IN} is positive. With the ganged switch position as shown (used for measurement on npn transistor) D_2 is ON and D_1 is OFF. Since D_2 conducts a virtual ground exists at the input of OP1. Because

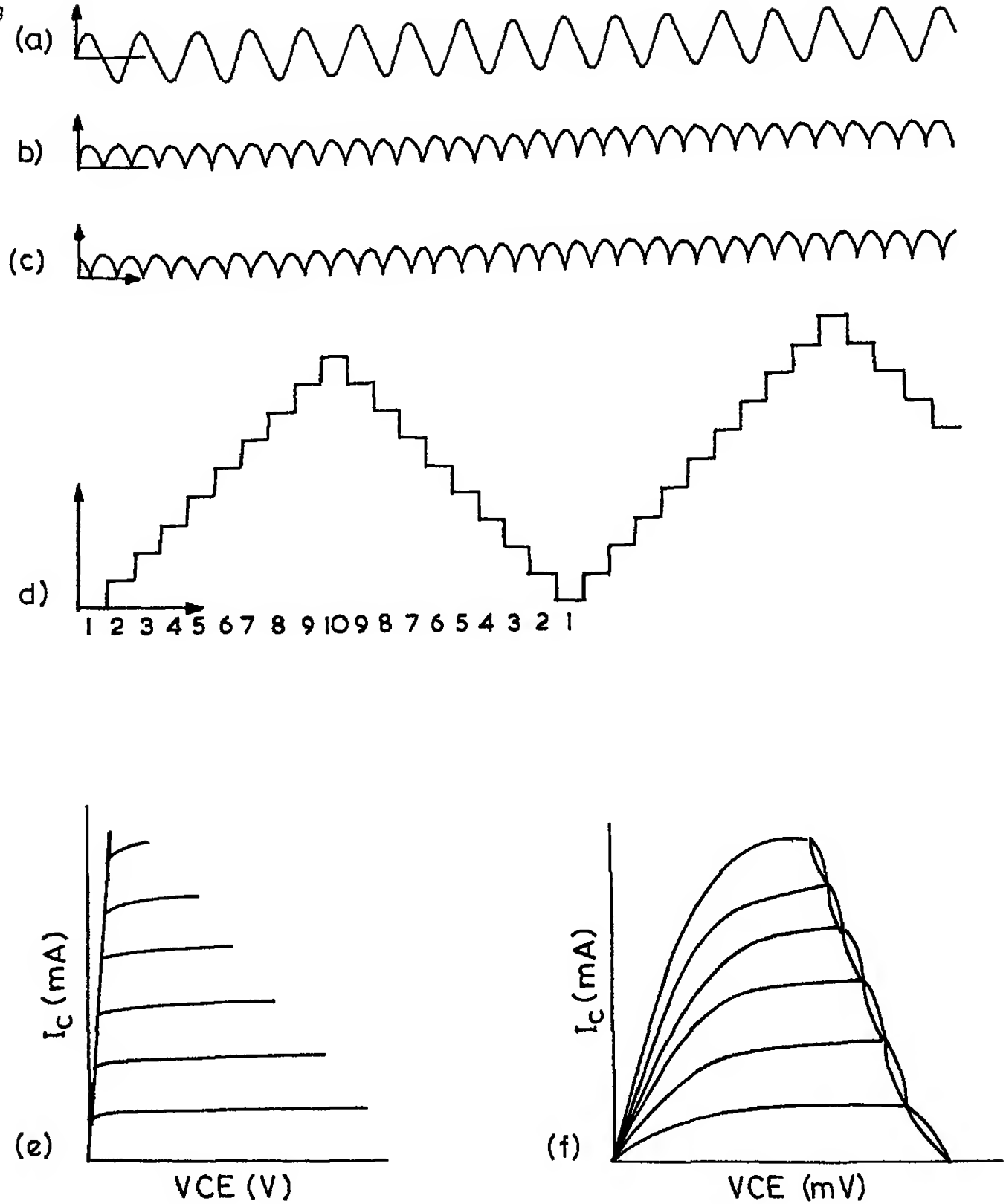


Fig 3 2(a) Input voltage waveform (b) Collector voltage derived from(a) Using ZCD (c) The same as (b) but using a 90 phase shifter preceding ZCD (d) I_C V_{CE} characteristics with collector voltage as in(c)

3 3 1 Collector Sweep Circuit

The system indicated in Figure 3 3 gives full wave rectification with/without inversion and with a gain R/R_1 controllable by one resistor R_1 followed by a current booster circuitry. This has the advantage over ordinary rectifier that it does not suffer from zero crossing distortion. If a sinusoidal voltage whose peak value is less than the cut-in voltage V (0.6 V) of a diode is applied to an ordinary rectifier circuit we get output to be zero for all the times. And for a low level signal there is appreciable phase lag in zero crossing. By placing the diodes in the feedback loop of an OPAMP the cut in voltage is divided by the open loop gain A_V of the amplifier ($V_{Y\text{eff}} = V_Y / |A_V| \approx 60 \mu\text{V}$ for $A_V = 10^5$) and the diode acts like an ideal rectifier. Though a straightforward modification of the ordinary rectifier (whereby each diode is replaced by an ideal diode so described and a summer is introduced at the end) is feasible but the choice of our circuit is obvious as in the former case each input OPAMP is strained by large differential voltage across its inputs and also it requires an extra stage a summer at the output. Moreover the gain is easily controllable in our adopted system by only varying the resistance R_1 .

The basic operation of the circuit is as follows. Let us consider first the half cycle where v_{IN} is positive. With the ganged switch position as shown (used for measurement on npn transistor) D_2 is ON and D_1 is OFF. Since D_2 conducts a virtual ground exists at the input of OP1. Because

D_1 is nonconducting there is no current in the R which is connected to the non-inverting input of OP2. Hence this input is grounded. The system then consists of two OPAMP in cascade with the gain of OP1 equals $(-R/R_1)$ and that of OP2 equals (-1) . The net result is

$$v_{OUT} = + R/R_1 v_{IN} \quad \text{for } v_{IN} > 0 \quad (3.1)$$

Consider now the negative half cycle of v_{IN} . This time D_2 is OFF while D_1 is ON. The inputs of OP2 stay at the same potential v . Since the negative input of OP1 is at the ground (virtual) potential, the Kirchhoff's current law at this node gives

$$\frac{v_{IN}}{R_1} + \frac{v}{2R} + \frac{v}{R} = 0 \quad \text{or} \quad v = -\frac{2}{3} R/R_1 v_{IN} \quad (3.2)$$

And that at the node (negative input of OP2) gives

$$\frac{v_O - v}{R} = \frac{v}{2R} \quad \text{or} \quad v_O = \frac{3}{2} v = -\frac{R}{R_1} v_{IN} > 0$$

$$\text{for } v_{IN} < 0 \quad (3.3)$$

where use is made of the previous expression (3.2). We thus see the outputs for the two half cycles are identical provided the four resistances R are perfectly matched. In actual practice using a variable resistance in place of R connected between S_2 and negative input of OP1 is enough to avert the problem that may arise because of mismatch of the resistors. The effect of input dc offset voltages and currents is more or less nullified by using the method discussed in Appendix I.

Since the output voltage is always positive this can be used as collector sweep voltage for npn transistor. With the ganged switch pushed to the other position ($S_1 \rightarrow A$ and $S_2 \rightarrow B$) enables one to use the same system for pnp transistor as here one gets inverted rectified output.

An OPAMP (we have used 741C) can provide a output current typically some 20-30 mA as a maximum. The high injection region of the transistor well exceeds this limit. So what we need is a current booster after this stage. The circuit is essentially an emitter follower with the OPAMP used at the input to get rid of the base emitter voltage drop suffered by the output voltage to be taken from the emitter point. The rating of this transistor should be greater than the rating of the transistor on which measurement has to be done. One can use field effect transistor (FET) as well. The switch (S) position is shown in Figure 3.3 while measurement is taken on npn transistor. For its complementary case - study the switch position connects negative supply to the pnp transistor so that the EB junction is always forward biased and negative feedback through the OPAMP is fulfilled.

When the output characteristic (I_C vs V_{CE} plot keeping I_B as parameter) is wanted the switch S_3 is to be connected with point E (as shown in figure) and then the collector series resistance includes the sampling resistance R_S also. For measurements like V_{be} vs I_b keeping V_{ce} constant V_{IN} comes from power supply (negative or positive supply depending on whether npn or pnp transistor is chosen).

the switch S_3 is connected to F R_C is shorted so that a constant voltage appears at the collector point whose magnitude can be specified by varying R_1 . Since R_3 now comes in the feedback loop its magnitude must be taken small. When ever the next base step (ΔI_B) comes the voltage at the output of the opamp or base of the power transistor suffers an instantaneous change of amount $V_T \ln(1 + \frac{\beta \Delta I_B}{I_C}) \approx R_3 \beta / I_B$ where β is the small signal gain. Slew rate of the OPAMP could then restrict this instantaneous change and for large collector current the output of OPAMP may get saturated unless a small R_3 is used. The best remedy for this problem is to use a power FET instead of the BJT and to place R_3 between the drain point and the supply point. Since there is practically no gate current the same current flows at the drain and source terminals and is again the (negative) input to the OPAMP. It draws no appreciable current. This is the same as the collector current itself.

3.3.2 Measurement section

The collector current is measured by sampling the difference voltage across R_3 and then dividing it by R_3 itself. This is nothing but the emitter current of the power transistor as the negative input terminal is not drawing any significant current. Two points are kept in mind while designing the instrumental amplifier. Firstly it should not draw any appreciable current from either input and secondly the common mode voltage rejection should be as far as possible. The first point is obvious. Second point arises because of the fact that there is a large exertion of common

mode voltage at the two ends of R_S whereas difference signal happens to be very small at lower base steps. One can use larger value of R_S but that would lead to other complications as has been just discussed. Popular instrumentation amplifiers take care of the first issue but fails to meet the second requirement.

A modified form is adopted here. As depicted in Figure 3.4 the input pair of LM110 (dedicated voltage follower) serves the purpose of a buffer stage. Voltage offset balancing is done as shown. One of the outputs is inverted so that the current due to difference signal alone is drained through R_F . The output voltage is then

$$V_O = R_F/R (V_2 - V_1) = R_F/R R_S I_C \quad (3.4)$$

The output voltage is thus proportional to I_C . With the choice $R_F = R = 1000 \text{ K}$, $R_S = 1000 \text{ K}$ the magnitude of V_O (in volts) gives the collector current in mA.

In choosing the OPAMPS LM108 is preferred because of its availability and its much lower offset drift than ordinary general purpose 741 type of OPAMPS. The necessary compensation is made. The circuit is tested with a common mode voltage as high as 10 V but with an output of 2-3 mV only whereas popular design ensures the common mode output not less than some 30 mV or so under the same condition.

N.B. It is to be noted that since the voltage V_2 is itself a regulated voltage source the upper follower (LM110) is redundant and it can be omitted as well. In that case if

LM108/LM110 have good delay matching $-V_2$ and $+V_1$ will be in good antiphase and hence this ensures better accuracy

3 4 BASE STEP GENERATOR

3 4 1 Synchronizer and Frequency Multiplier

As has already been discussed in Section 3 2 a base step change should occur at the beginning of every collector sweep (i.e. for $V_S = V_{CC} - 0$) so that a neat display of the family of curves will be obtained. But if we are interested in the saturation (low V_{ce}) region than the noisy scene close to $V_{ce} = 0$ that arises because of imperfect synchronisation may not enable one to extract good reading from that region. It is then advisable to make the occurrence of base steps when applied voltage V_{CC} and hence V_{ce} is at its peak. The type of display we will get is shown in Figure 3 2(a). Due to charging and discharging of parasitic capacitances some uncharacteristic traces or loop would be formed at the far end of the curves a region which we are not interested for low V_{ce} I_C measurement. Anyway the modification that we require for the latter case is to use a 90° phase shifter preceeding the zero crossing detector. This part of the circuit is shown in Figure 3 5.

With the ganged switch position shown ($S_4 \rightarrow 4$ and $S_5 \rightarrow 2$) the input OPAMP (OP4) is activated as an integrator with a transfer function given by [3]

$$A_{vf}(s) = -\frac{s_1}{RC} A_{vo} \frac{1}{(s + A_{vo}s_1)(s - 1/RC A_{vo})} \quad (3.5)$$

where A_{vo} is a negative number being the open loop voltage gain and s_1 the dominant pole of the OPAMP in absence of C

The transfer function has two poles on the negative real axis as compared to a single pole at the origin for the ideal integrator. We observe that the performance of the real integrator departs both at low and high frequencies. At high frequency the integration is limited by the finite bandwidth ($-S_1/2\pi$) of the operational amplifier while at low frequencies the integration is limited by the finite gain of the OPAMP. For $\mu A741$ $A_{VO} = 10^5$ $f_1 = 10$ Hz and since our f is limited between 200 Hz to 1.5 kHz the expression (3.5) reduces to

$$A_{vf}(S) = -\frac{1}{RCs} \quad (3.6)$$

hence an ideal integrator. The choice of RC is defined by the attenuation wanted. With the same resistance R applied to positive input only input offset current I_{IO} flows through capacitance. The resistance R itself has to be chosen low enough so as to mask the effect of offset current and offset voltage. We have chosen $R = 10$ k $C = 0.05$ μF so that $|A_{vf}| = 2$ for $f = \frac{\omega}{2\pi} = 636$ Hz. Its variation between 1 to 3 (roughly) for the operating frequency range 300 to 1 kHz is alright as we are interested only in the phase shift and subsequent stage have nothing to do with the magnitude of the voltage.

With the ganged switch rotated to the other position ($S_4 \rightarrow 1$ $S_5 \rightarrow 2$) the integrator circuit is isolated and it is in fact modified to a mere voltage follower output always sitting at zero volt because of feedback action through R.

Now v_{IN} is directly connected to the next stage a zero crossing detector. Since we aim to get pulses at both positive and negative going zero crossings we choose LM361. It is a high speed differential input comparator [1] with complementary TTL output voltage levels. It provides independent strobing facility for the complementary outputs and can be operated over a wide supply voltage range. It guarantees low input offset voltage and tight delay matching on both outputs.

The complementary outputs are individually sent through a simple RC differentiator and then through a diode to clip off the negative spikes. The value of R is chosen so that the spikes are sufficiently high and the selection of C is dictated by the demand that the time constant RC should be small so that the tail drops close to zero before the next spike comes. The choice $R = 51\text{ k}$ and $C = 1\text{ }\mu\text{F}$ gives good performance. The outputs of the diodes are then sent through inverters to purify the pulse shape and then through NOR gate. Pulses are interdigitated at the final output. The latter thus has frequency twice the frequency of the individual ones.

For the two inverters and the final NOR gate three fourth of a 74C02 (quad two input CMOS NOR chip) is used. Here choice of CMOS gate is essential as with input resistance 51 k the input of TTL inverter gate would never go to lower logic level. Improper choice of R and C in the differentiator circuit aging or hardware troubles may

distort the shape/levels of the output pulses To rectify this a level detector can be inserted with the other input of the comparator maintained at 2.4 V

3.4.2 Triangular/Sweep Generator

The circuit for this part is shown in Figure 3.6 The digital output (with frequency twice the frequency of the input sine wave) of the previous stage is applied to the clock input of 74191 It is a binary counter with DOWN/UP mode control active low LOAD ENABLE control inputs It gives an output pulse R_C at the pin no. 13 which goes low for half of the clock period before overflow/under flow occurs The digital outputs of the counter are fed to the DAC so that we would get a digitised waveform depending on the control logic used to the counter For example keeping LD = HIGH EN = LOW and DN/UP permanently at high or low we would get negative going or positive going sawtooth wave But the sharp fall of output corresponding to transition 1111 \rightarrow 0000 (or the reverse for negative going sawtooth) may give rise to glitches or other hardware problems So we prefer to use it as a triangular wave generator This can be done by controlling DN/UP mode control as shown in figure The negative going edge of the ripple clock R_C is used to clock the toggle switch (made from JKFF by holding both J and K input at high) whose Q output is connected to PIN5 (DN/UP) of 74191 Consider the situation when DN/UP = 0 the system is counting up When the outputs Q_A , Q_B , Q_C and Q_D of the counter attain 1111 the ripple clock goes low which forces the DN/UP

input to go to 1 since $R_C = \overline{\text{CLK}} \text{ MX/MN } \overline{\text{EN}}$ while $\text{MX/MN} = \overline{\text{DN/UP}} Q_A Q_B Q_C Q_D + \text{DN/UP } \overline{Q_A} \overline{Q_B} \overline{Q_C} \overline{Q_D}$. The latter transition in turn forces R_C to go high again after a few delays. Any way since DN/UP now latches at high state the counter will start down counting (1111 \rightarrow 1110 so on). Before reaching the state 0000 the low going transition of R_C will again change the counting state. We will thus get a triangular wave.

The first one of the DACs in the system is simply used as digital to analog converter whilst the next one is basically used as an attenuator to get a wider range of base steps. In fact a single chip like AD390 can be used to attain both the functions but we have not used them because of their immediate non-availability to us. DAC08 is a TTL compatible 8 bit DAC. It works upto ± 10 V reference with two quadrant wide range multiplying capability. It is highly linear and gives complementary current outputs $I_{\text{OUT}} + \overline{I_{\text{OUT}}} = I_{\text{FS}}$ for all logic states where $I_{\text{FS}} = \frac{255}{256} \frac{I_{\text{REF}}}{I_{\text{REF}}}$ (see Figure 3.6). These currents are sinking currents so that for taking measurement on pnp transistor I_{OUT} (with $\overline{I_{\text{OUT}}}$ pin grounded) current can be directly connected to the base of the test transistor. And to apply negative base step voltage a load resistor R_L ($= 10 \text{ k}$) is applied between PIN4 and ground (with pin2 ground) and then using a voltage follower to buffer this voltage. The range of the voltage step available would be from 0 to $-I_{\text{FS}} R_L$. Since we are interested in testing npn transistors also the output is connected in the inverting

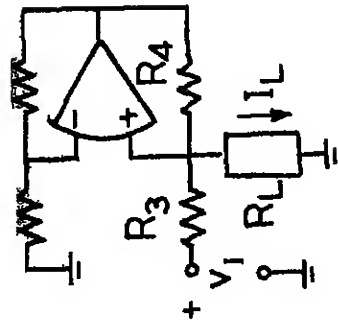


Fig 37a VCCS using single OPAMP

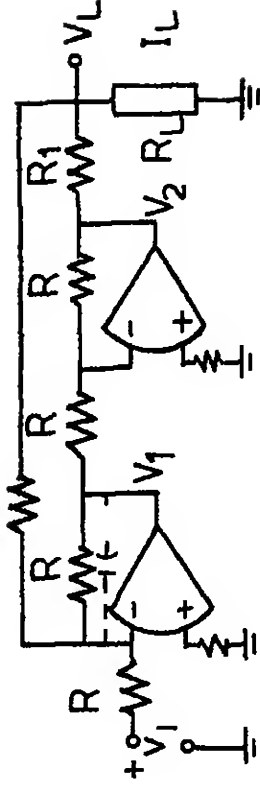
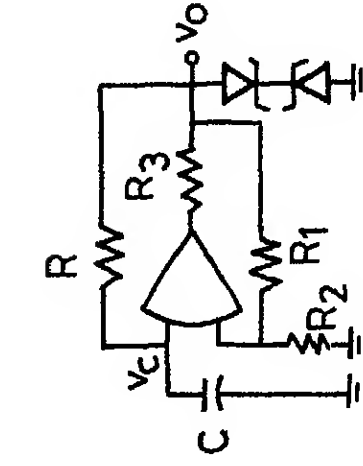
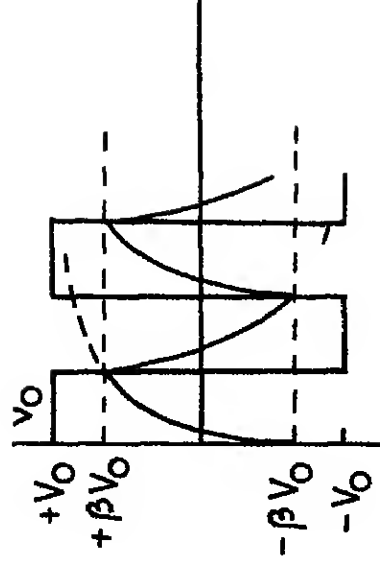


Fig 37b VCCS using double OPAMPS



(a)



(b)

Fig 38(a) Astable Multivibrator (b) Waveforms across the output and across the capacitor, $\beta = R_2 / (R_1 + R_2)$, $V_0 = V_Z + V_D$ and $R_3 > (V_{OH} - V_0) / I_{sc}$

mode (as shown) so that one gets inverted positive output within the range 0 to $+I_{FL}R_L$. This voltage step then can be directly applied to the test transistor (npn) base for taking I_C V_{be} measurement. To get a current step from this voltage step we have passed it through a VCCS.

The VCCS that we have implemented here (Figure 3 7b) is somewhat different from the standard type (Figure 3 7a) using a single opamp for grounded load configuration. The latter suffers from the disadvantages firstly of poor common mode voltage rejection; secondly the output resistance of the controlling voltage source influences the adjustment and in addition the current supplied by the control-voltage source is dependent on the load resistance; thirdly any imperfect matching of the resistances R_1 , R_2 , R_3 & R_4 degrades the output shunt resistance of the current source appreciably. Our circuit is more favourable in these respects.

To analyse the operation of the circuitry (Figure 3 7b) we note that the second opamp is simply acting as a voltage inverter. So applying KVL for the circuit we get

$$V_2 = -V_1 = V_1 + \frac{R}{R_2} V_L \quad (3.7)$$

The application of KCL to the output gives

$$\frac{V_2 - V_L}{R_1} - \frac{V_L}{R_2} - I_L = 0 \quad (3.8)$$

Elimination of V_2 from (3.7) and (3.8) yields

$$I_L = \frac{V_1}{R_1} + \frac{R - R_2 - R_1}{R_1 R_2} V_L \quad (3.9)$$

The output current will be independent of output voltage if the condition

$$R = R_1 + R_2 \quad (3.10)$$

is satisfied

In our design we have chosen $R_2 = 10\text{ k}$ the resistances R_1 and R_2 are derived from a single 10 k pot so that $R_1 + R_2 = 10\text{ k} = R_2$ is satisfied. Input dc offsets are appropriately taken care of. A small capacitor (100 pF) is applied to the input OPAMP (shown in figure) to avoid oscillation. Note that the choice of low R_1 (and hence I_L) is restricted by the output current drive requirement of the second opamp. Again choice of high R_1 (and hence low R_3) may create excess voltage drop across it and the opamp may get saturated (this is also evident from (3.7)). The usable range of R_1 for a given v_{imax} can be worked out.

3.5 CONCLUSION

The circuit design we have discussed so far is assembled and the system worked out well. It ensures precision measurement which is so important for modelling second order effects. For example in the I_C - V_{CE} characteristics with I_B held constant I_C normally shows a slight upward slope in the active region because of Early effect (vide Section 2.3). Now even quite a small variation of I_B is sufficient to mask this effect. Hence a constant current source is mandatory. Many variations of the circuit are possible. Suppose if one wants to display single or a restricted set of

curves that can be done by proper logic connections to LD and UP/DN input of the counter. The only disadvantage of the design is that it requires a signal generator. This dependence can be omitted by the simple additional design as sketched in Figure 3.8. The output symmetrical square wave as before has to be processed through ZCD in order to make it TTL compatible. The charging and discharging voltage v_c across the capacitor is first buffered and then can be used as input voltage v_{IN} to Figure 3.5 as any periodic waveform is sufficient and its shape is unimportant. Or one can derive the waveform from power line itself via transformer or variac. Though not meant for this system can also be used for monitoring other devices like MOSFET, JFET etc by suitably connecting to appropriate outputs.

CHAPTER 4

FORMULATION OF THE MODEL

4.1 INTRODUCTION

Modelling is the art of characterisation of the behaviour of a physical process. The device model attempts to describe the terminal electrical behaviour of the device and the user need not know the internal physics. There are many ways of approaching this problem depending on one's knowledge on the internal mechanism and on the measurement techniques. In case one has little idea about the system one can propose an empirical model and the parameters of the model can be obtained from experimentally measured behaviour of the device as viewed from its terminals. This involves application of curve fitting techniques to obtain functional relationships between the terminal quantities of interest. The result itself may help the user to get insight into the system. But the problem in using this type of model is that the operating and environmental conditions are identical to those under which the measurements have been made. The physical model on the other hand is based on the analysis of the basic internal physical mechanisms and the parameters chosen naturally would be related to material and structural properties of the device. Hence the model equations would themselves remain canonical with respect to changes in operating conditions as the exogenous variables (e.g. temperature)

are automatically taken into account. In other words, with known terminal behaviour, they enable the user to extract the information on the operating condition also.

A third class of techniques that we can think of (of course, after the advent of digital computers) is most robust and begins with the basic set of equations (like continuity equations, Poisson's equations, current equations, etc.) along with suitable boundary conditions. Though the solution seems to be most exact, it values a lot of computer time and memory, often making it unviable and unrealistic. As far as device people and design people are concerned, this does not provide any substantial benefit. The model we have described so far is a physical model developed from the behaviour of semiconductors at the junctions and the bulk regions.

In short, our approach would be like this. The transistor operation in different well-defined regions is considered. Different approximations valid for the respective regions are called for to attain analytic expressions. These are then solved on the computer. The computer result is monitored at various stages to check the self-consistency of the approximations and to check whether there is any hidden critical assumption that may arise in the model to diverge from reality (validation process). These demand a particular set of experiments in a particular region of operation which provides the input data. Anyway, the parameters extracted from a typical set may be required to be

used to find out its associated parameters in another run. Hence some sequences have to be maintained and one may have to iterate amongst various stages. In Appendix V we shall first discuss the least square curve fitting method (Levenburg-Marquard algorithm). In Section 4.3 we will first summarize the basic equations borrowed from Chapter 2 and discuss the relevant experimental techniques. In Section 4.3 we will show the way to exploit the more sophisticated model. Before completion we will indicate the compatibility with the existing SPICE simulation program.

4.2 MODEL EQUATIONS ELECTRICAL MEASUREMENTS AND EXTRACTION OF MODEL PARAMETERS

A model is of little use if acquisition of model parameters is difficult. In this section we shall discuss a list of simple dc and ac measurements along with the necessary set of equations that are sufficient for the extraction of the model parameters. Each set of measurements tends to emphasise a separate physical effect and allows extraction generally of three to five model parameters. In cases where a physical effect is significant in more than one set of experiments an iterative process is necessary. For our case we take 2N2219 as the test transistor. It is a medium power switching transistor and can be used as an amplifier also. Some sets of data have been taken straight away from the data book [5] for the verification of the software developed.

4 2 1 C_e as a Function of V_{BE} and C_c as a Funct on of V_{BC}

As has been pointed out at the beginning of Section 2 3 1 the usual expression of junction capacitance given by (2 19) suffers from singularity This has been bypassed in the proposition of (2 19a) So if one takes its derivative the following result is evident

$$C_e = \frac{C_{oe}}{(x^2 + b)^{n_e/2}} \left(1 + \frac{n_e}{1 - n_e} \frac{b}{x^2 + b} \right) \quad (4 1)$$

where $x = (V_{BIE} - V_{BE})/V_{BIE}$ The elements of the vector P in (2 19) is then given by

$$p_1 = V_{BIE} \quad p_4 = b; \quad p_2 = n_e/e \quad \text{and} \quad p_3 = \frac{C_{oe} V_{BIE}}{1 - n_e} \quad (4 1a)$$

The initial choice of the parameters are important A rough estimate for them can be obtained as follows One may use $V_{BIE} = V_T \ln \frac{N_E N_A}{n_i^2}$ or it can be assigned the default value 0.7 V in case the doping levels are not know n_e (cal ed the grading factor) is estimated from the slope of $\ln C_e$ versus $\ln(1 - V_{BE}/V_{BIE})$ C_{oe} is the measured zero bias capacitance A forward biased capacitance C_{ef} can be estimated from the extrapolation of the slope of the reciprocal cut off frequency such that

$$C_{ef} = \frac{V_T}{2\pi} \frac{d(1/f_T)}{d(1/I_C)} \quad (4 2)$$

a_{e2} is related to C_{ef} by [39]

$$b = \left[\frac{(1 - n_e) r C_{ef}}{C_{oe}} \right]^{-2/n_e} \quad (4.2a)$$

where r is constant close to unity. Its exact value depends on doping profile. These estimated values can be used as initial guesses for a non-linear curve fitting procedure which fits the measured values of C_e to the calculated values by adjusting V_{BIE} , n_e , C_{oe} and a_{e2} according to (4.1). Note that the parameters finally obtained are purely model parameters though they can be attributed to physical definitions as discussed above.

By a similar procedure one can calculate V_{BIC} , n_c , C_{oc} and a_{c2} and in turn the elements of P_c . But before that one thing is to be noted. The measured terminal capacitance is the total capacitance $C_t (= C_c + C_1)$ whereas C_c represents the capacitance of the active part of the base-collector junction. Anyway all the relations in (4.1a) can be used excepting the third one which should be modified to be

$$P_3 = \frac{C_{oc} V_{BIC}}{1 - n_c} \cdot \frac{1}{1 + r_A} \quad (4.1b)$$

where r_A is defined in (2.123a)

4.2.2 n_{FE} Versus I_C (At Low Injection)

In Section 2.2 we have deduced the basic equations relating junction voltages with currents. In the normal active mode equations (2.10) and (2.13) reduces to

$$i_C \cong i_{CC} \cong i_S e^{V_{be}/q_b} \quad (4.3)$$

and

$$i_b = i_S / \beta_F e^{v_{be}} + i_{SE} e^{v_{be}/\eta_e} \quad (4.4)$$

where currents and voltages are in normalised form (e.g. $i_C = I_C/I_k$ etc and $v_{be} = V_{BE}/V_T$) Eliminating $e^{v_{be}}$ from them we get the following useful expression

$$\frac{1}{h_{FE}} = \left| \frac{i_b}{i_C} \right| = \frac{q_b}{\beta_F} + i_{SE} (i_C q_b)^{1/\eta_e} / i_C \quad (4.5)$$

$$\text{where } i_{SE} = i_{SE} i_S^{-1/\eta_e} \quad (4.5a)$$

This relationship can be utilised to extract the parameters I_k , β_F , i_{SE} and η_e from h_{FE} versus I_C curve provided we have the knowledge on q_b before hand. For this we take the equation (2.9) divide throughout by Q_{bo} and assuming $Q_{bo} = \tau_F I_k$ (by definition of I_k) we end up with the following expression for q_b

$$q_b = 1 + q_{be} + q_{bc} + B i_C \quad (4.6)$$

where we have neglected the last term. The expression for q_{be} and q_{bc} are available in (2.20) and (2.21). The relevant parameters (P_e , P_c) has already been extracted from reverse capacitance voltage curve (see Section 4.2.1). The only unknown quantity left is B . By carefully choosing (I_C , V_{CE}) points such that I_C remains less than the critical current I_0 (function of V_{CE} see Section 2.3) at which base push out effect starts occurring enables us to put $B = 1$.

After getting the above four parameters we now concentrate on the tail portion of the $h_{FE} I_C$ curve where the base push out effect is predominant. By introducing appropriate expression for the factor β in (4.6) the characteristic parameters are then amenable for numerical evaluation. But the push out effect also comes into play in the experiments (4.2.3) and (4.2.5). This means that data from these measurements have to be fitted alternatively until a consistent set of model parameter is obtained. We shall describe the procedure in Section 4.3.1.

4.2.3 Measurement of Emitter and Collector Series Resistances

Shockley et al [42] have indicated that for an ideal transistor in the common base configuration the floating ($I_C = 0$) collector to base voltage will be almost identical to the forward biased emitter to-base voltage. But in an actual transistor the difference between the two voltages is attributed to the volume recombination of carrier pairs which diffuse from emitter to the collector. Accordingly in an ideal transistor in a common emitter orientation $V_{CE}|_{I_C=0} = 0$ whereas in an actual transistor with emitter series resistances R_E $V_{CE}|_{I_C=0} \approx -R_E I_E = R_E I_B$. Similarly if the emitter and collector are interchanged to operate in common-collector orientation then with a collector series resistance $R_{CC}(=R_C + R_C)$ $V_{EC}|_{I_E=0} \approx -R_{CC} I_C = R_{CC} I_b$.

Thus measurement of floating collector and emitter voltages as a function of forward biased base current will provide evaluation of R_E and R_{CC} . These measurements have been done by our curve tracer as follows. The base current step is as usual applied to provide the forward biasing whilst emitter is grounded and the collector is kept floating. Then the collector and emitter (ground) points are connected to the measurement unit (see Section 3.3.2) to measure the voltage (V_{CE}). This ensures a high impedance ($\sim 1 \text{ G}\Omega$) essential for such measurement. For measurement of R_{CC} the above connection has to be made in reverse. Then from the display the slope of the lines would give R_E and R_{CC} .

4.2.4 I_C as a Function of V_{BE} at Constant V_{CE}

If the convention for terminal current that all current flowing in is positive is adopted then the terminal BE voltage is related with true junction voltage by

$$V_{BE} = V_{BE} - I_b(R_b + r_b/q_b) + I_E R_E \quad (4.7)$$

where $I_E = -(I_C + I_b)$ is the emitter current. The symbols have their usual meanings. Combining (4.7) with (4.3) we get

$$V_{BE} = V_T \ln[(I_C/I_S)q_b] + I_b(R_b + r_b/q_b + R_E(1 + h_{FE})) \quad (4.8)$$

If I_b is not measured along with I_C then one can use I_C/h_{FE} instead of I_b in (4.8) where h_{FE} is to be taken either from previous experiment or through the use of (4.5) since parameters like I_K , η_e , β_F , I_{SE} are already known. Equation (4.8)

can be subjected to curve fitting technique to squeeze the parameters V_T , i_s , R_b and r_b . R_E is very small normally of the order of 1Ω (the contact lead resistance). Note that we have not accepted a standard value of V_T (25.9 mV at 300 K). Since the operating temperature is unknown and it appears in the exponent it has got significant effect on the magnitude of the current and thus there is enough justification to take it as a model parameter. At low injection $q_b \approx 1$ and it is not possible to get R_b and r_b separately (because of lack of sensitivity) rather their sum $R_{bb} = R_b + r_b$ should be taken as a single model parameter. At high currents where the base resistivity modulation is significant one can use the same equation (4.8) to extract r_b alone accepting the already known above parameters.

4.2.5 Output Characteristics (V_{CE} versus I_C) in Saturation Region

Here the EB as well as CB junction are forward biased. Hence both of them have significant role on the currents in the system. For the time being we are neglecting the contribution from overlap diode and conductivity modulation in the collector region. We consider the following set of equations (4.7), (2.13), (2.64), (2.10) and the two given below

$$V_{bc} - V_{be} + V_{ce} = 0 \quad (4.9)$$

$$V_{bc} - V_{bc} - (R_b + r_b/q_b)I_b + (R_c + R_c)I_c = 0 \quad (4.10)$$

These comprise of six equations with eight variables. Given I_b , V_{ce} these equations can be solved for the other four

variables All the constants barring β_R , I_{SC} , η_C , τ_t are already known Using their known values and accepting some initial value for the remaining four one can solve the above set of equation in a manner already prescribed The calculated value of I_C is then compared with the measured value until best fit is obtained The parameters are updated in each iteration until the convergence is reached Alternatively one can extract the same four parameters by going to inverse active region and then adopting a procedure similar to that written in Section 4 3 2

4 2 6 f_T as a Function of I_C at Constant V_{CE}

This experiment can provide a lot of information for high frequency and transient operation of a transistor and also it helps to determine the model parameter of base push effect But there exists a lot of confusion [38 39] about the exact definition of f_T and the way it has to be measured Hence a clear understanding of f_T is necessary

Let us define the transit frequency f_T as

$$f_T = |\beta| f \quad (4 11)$$

where β = short circuit common emitter current gain

From this it is to be seen that if $|\beta|$ varies inversely with frequency (or it falls with 6 dB per octave) then f_T is independent of frequency and it equals to f_{T0} the unity gain frequency If this approximation is valid then it is easy to measure f_{T0} by measuring β at any high frequency and then taking help of (2 11) But we shall see below that

the permissible frequencies for this measurement are restricted to a certain range

The conventional expression for the low frequency dependence of β

$$\beta = \frac{1}{1/\beta_0 + j 2\pi f \tau} \quad (4.12)$$

where τ is the emitter to collector delay time. Writing $1/f_\beta$ for $2\pi\tau$ the modulus form of (4.12) appears as

$$|\beta| = \beta_0 \sqrt{1 + (f/f_\beta)^2} \quad (4.12a)$$

Here f_β physically stands for 3 dB cut-off frequency. Defining the ideal transit frequency by

$$f_{TO} = \beta_0 f_\beta \quad (4.13)$$

We get the following relation to f_T from (4.11)

$$f_T = \frac{f_{TO}}{\sqrt{1 + (f_{TO}/f \beta_0)^2}} \quad (4.14)$$

We can at once conclude about the lower limit of the usable frequency range. Assuming $(|\beta|/\beta_0)^2 \ll 1$ we see from (4.12) and (4.13) $(f_{TO}/f \beta_0)^2 = (f_\beta/f)^2 \ll 1$ and equation (4.14) reduces to $f_T = f_{TO}$. Thus the measuring frequency chosen should be at least some five to six times larger than f_β . The upper limit to it (over which f_T will again become frequency dependent) is caused by parasitic transistor and package parameters i.e. they contribute to higher order poles and zeros which are far ^{lower} than the cut-off frequency f_{TO} .

itself This limit is calculated in a laborious way in the paper [40] and also the optimum frequency is suggested

Let us now turn our attention how to extract information from the f_T versus I_C curve One can define the emitter to collector transit time

$$\tau \cong \frac{dQ_T}{dI_C} \quad (4.15)$$

where Q_T represents the total excess majority charge in the emitter base and collector junctions and quasi-neutral regions. Using quasi-neutral condition one can also equate excess majority carrier charge with the excess minority carrier charge In the active base region the model charge is Q_b And its derivative with respect to I_C gives the following terms

$$\begin{aligned} \frac{dQ_b}{dI_C} = & (C_e + C_c) \frac{q_1 V_T}{q_b I_C} (1 + 2q_2/q_1) \\ & + C_c [(R_b + r_b/q_b)/\beta + R_E + R_C + R_C] + B \tau_f \end{aligned} \quad (4.16)$$

where we have taken help from (4.3) (4.9) and (4.10)

$q_b = q_1 + q_2$ all other symbols are already defined

(Actually τ_f to be replaced by τ_{fN} where $1/\tau_{fN} = 1/\tau_f + 1/\tau_b$ where τ_b is the recombination life time in the base) Note that this is valid at both low and high injection If we take into account the capacitive effect of the inactive base region it provides an additional delay

$$\frac{dQ_1(V_1)}{dI_C} = C_1(V_1) \frac{dV_1}{dI_C} \quad (4.17)$$

where C_1 is defined in (2.123) and V_1 is given by

$$V_1 = V_{bc} + (r_b/q_b)I_b + R_C I_C \quad (4.18)$$

then (4.17) can be evaluated to be

$$\frac{dQ_1}{dI_C} = C_1 \left[\frac{q_1 V_T}{q_b I_C} (1 + 2q_2/q_1) + R_C + R_E + R_b \right] \quad (4.19)$$

If we sum up (4.16) and (4.19) and also include in that the parasitic capacitance C_{pe} between the emitter base terminals (it consists of the capacitance of the bond pads of the package and possibly of the measuring socket) which acts in parallel to C_e we end up with

$$\tau = \frac{1}{2\pi f T_O} = B \tau_{fN} + C^* \frac{q_1 V_T}{q_b I_C} (1 + 2q_2/q_1) + \tau_c + \frac{w}{2v_s} \quad (4.20)$$

$$\text{Here } C^* = C_e + C_c + C_1 + C_{pe} \quad (4.20a)$$

$$\begin{aligned} \tau_c = & (C_c + C_1)(R_C + R_E + R_b/\beta) + C_c(R_C + \frac{r_b}{q_b\beta}) \\ & + C_{pe}(R_E + [R_b + r_b/q_b]/\beta) \end{aligned} \quad (4.20b)$$

The last term in the expression (4.20) incorporates the delay time in CB junction depletion layer w is the depletion width given by (2.24) v_s is the saturation velocity. Usually this term is very small and can be neglected.

Let us try to explain Figure 4.1 in the light of (4.20). The shape of the curves reports three physical effects. At low collector current f_T is dominated by the second term in (4.20) which is approximately $C V_T/I_C$. At

low collector current the difference in f_T between the cases with $V_{CE} = 5$ V and with $V_{CE} = 10$ V is resulted mainly from the first term in (4 20b). The maximum f_T is limited by τ_f which is roughly $w_b^2/2\eta D_n$. At high collector currents base push out effect causes rapid decrease in f_T . Hence at low I_C but different V_{CE} data on f_T helps in determining R_C since $C_t (= C_C + C_j)$ is already known from (4 1) at intermediate values of I_C an estimate of τ_{fN} is possible. From the f_T I_C (large) data the model parameters of base push out effect can be found out.

As already mentioned at the beginning of this subsection a necessary condition for determining the parameters from the measured curve $f_T(I_C) = |\beta| f$ (equation (4 11)) in the manner described above is $f_T = f_{T0}$ with f_{T0} from (4 20). That means f_T must not depend on the measurement frequency within a certain current range. First of all we note that for a diffusion transistor the transport factor $\alpha_T = \text{sech}(w_b/L_b)$ the frequency dependence of $\alpha(w)$ is therefore given by $\alpha(w) = \text{sech} \frac{w_b}{L_b} (1 + jw \tau_b)^{1/2}$ where the base diffusion length is replaced by its complex value $L_b^* = L_b / (1 + jw \tau_b)^{1/2}$. In view of the relation $\beta(w) = \alpha(w) / (1 - \alpha(w))$ we see that $\beta(w)$ is no longer given by (4 12) rather it is approximately valid if one expands the sech term and retains the first two in the series. When base grading is present an empirical expression is proposed:

$$\alpha(w) = \frac{\alpha_0}{1 + jw/w_g} e^{jmw/w_g} \quad (4 25)$$

where $w = 2\pi f$ is the operating angular frequency with

$$m = 0.22 + 0.1\eta \quad (4.25a)$$

$$\text{and} \quad w_\alpha = \frac{2.43 D_b}{w_b^2} [1 + (\eta/2)^{4/3}] \quad (4.25b)$$

At low w the exponential term in (4.25) reduces to unity and again (4.12) can be realised. At high frequencies the origin for the strong dependence also comes from parasitic lead inductances and stray capacitances. Figure 4.1 clearly displays this feature. It is also obvious in the low frequency range f_T is nearly independent of frequency and $1/2\pi f_T$ increases almost linearly with $1/I_C$ in accordance with (4.20). At high frequencies however f_T increases strongly with f . The results for $\beta_o = 50$ and $\beta_o = \infty$ are included in the same figure. Since the frequency chosen is low enough to avoid high frequency effect the curve with $\beta_o = \infty$ shows $f_T = f_{T0}$ (in view of (4.14)) and hence an ideal one. We therefore note that the best choice of frequency range is 0.3 to 0.5 GHz for this high frequency transistor. We also note that since high frequency effects start becoming significant at much lower frequencies than f_{T0} itself (i.e. the presence of secondary poles at much lower value than f_{T0}) the actual unity gain cut-off frequency significantly differs from (4.20) and also the phase lag is considerably different.

So far we have not included the storage charge effect in the emitter and collector regions. In the emitter region it creates a delay $\tau_e \approx Q_{pe} g_{be} / I_p(0)$ where Q_{pe} is the

excess minority carrier and $I_p(0)$ is the hole current in the emitter and g_{be} represents the ratio of the effective Gummel number in the E and B regions respectively. The expression is evaluated and found out to be

$$\tau_e = \frac{1 - f^{-1}}{\eta} \frac{N_A w_b}{N_E D_n} L_p q_b \frac{\text{sech}(w_E/L_p)}{\coth(w_E/L_p)} \quad (4.26)$$

The collector storage effect is important in saturation and inverse active mode operation. We have seen in (2.93) that charge density falls linearly with distance so that $\frac{p(0)}{p(x)} \approx \frac{w_{CIB}}{x}$. Using this approximation in the third term of (2.86) multiplying throughout by qA_c and then integrating over the limit $x = 0$ to $x = w_{CIB}$ (over which conductivity modulation is important) we get

$$Q_{CE} \approx \frac{1}{2} qA_c (p(0) + N_{ep}) w_{CIB} \quad (4.27)$$

taking the approximation $p(0) \gg N_{ep}$ and utilising the relationship (2.87) we get an approximate form of the collector storage delay

$$\tau_d \approx \frac{Q_{CE}}{I_C} \approx \frac{w_{CIB}^2}{4D_n} \quad (4.28)$$

where w_{CIB} is to be chosen from (2.95). These two delays (τ_e and τ_d) have to be included in (4.20).

One fact has missed our consideration so far we have neglected the last term since v_s is large. But at high current densities the electric field in the depletion region reduces because of Kirk effect and appropriate expression for carrier velocity ought to be used from (2.66) to (2.68).

instead of using v_g only. Hence this term gives rise to some contribution to the total delay at high collector currents.

Before passing we should mention that the software that has been developed is not based on the closed form expression (4.20). Rather the set of six equations mentioned at the beginning of Section 4.3.5 along with (4.18) where $Q_T = Q_b + Q_i$ are picked up. They include eight equations in 10 variables (V_{BE} , V_{BE} , V_{BC} , V_{BC} , V_{CE} , I_b , I_C , V_i , Q_b , Q_T). Given I_C and V_{CE} they are solved for by N-R techniques for the remaining eight variables. Furthermore the first derivative in (4.15) can be computed. By adjusting the value of the model parameters the calculated value of f_T is fitted to measured values. The parameters extracted will be discussed in the next section.

4.3 MODELLING ON THE BASIS OF EXTENDED GP MODEL

In the previous section we have discussed the method of measurement and extraction of pure GP parameters. In this section we shall take the help of the same set of measurements with one or two new additions to compute the relevant parameters. We have prescribed in Section 4.3.1 to make junction capacitance-voltage measurements and thereby to extract the parameters (P_e , P_c) which are required to model Early effect. We shall set aside these parameters and instead include V_{PIF} , V_{PEF} and V_{PIR} defined in equation (2.26) (2.32) and (2.37a) respectively as the model parameters for the same. Consequently the set of measurement one has to make radically gets changed.

The measurement of V_{rep} is done indirectly. A slow ramp is applied to the reverse CB junction while its capacitance is monitored. At voltage V_{rep} and more than V_{rep} the reading should show a constant value because the depletion region in the collector side touches heavily doped (n^+) substrate and to the base side it is going along upgrading. Hence the onset voltage for constant C_C should be identified with V_{rep} . This experiment is performed using PAR410 ramp generator with HP7015B XY Plotter for recording.

Measurement of V_{PIF} is directly possible if this voltage is less than CB junction breakdown voltage (BV_{CEO}). In that what have to do is to short the EB junction and increase V_{CB} (reverse) until the base depletion edge touches the EB junction. The CE current will show a steep rise at this voltage (V_{PIF}) which can be monitored. In case it is not possible one then can estimate it from the slope of $I_C(0)/I_C$ versus $\sqrt{V_{CB} + V_{BIC}}$ curve where $I_C(0)$ refers to collector current at $V_{CB} = 0$. The parameter V_{PIR} is not so much important and one can follow the same procedure as is used for the determination of V_{PIF} . Note that the determination of V_{PIF} , V_{rep} allow the determination of Q_{bo} , N_{ep} and w_{ep} . They can be found from CB junction measurement also but the parasitic effects impair accuracy.

One point we want to elaborate here is that the expression for $q_{bc} (= \frac{Q_{bc}}{Q_{bo}})$ that would be obtained from (2.33) or (2.34) as it suits should be inserted in (2.42) to get effective normalised charges associated with CB junction.

With slight change we rewrite this expression here

$$q_{bc \text{ eff}} = \frac{\left(\frac{N_r}{1-f^{-1}}\right)^\alpha (1+\alpha) \left(1 - \frac{C_F V_T}{E_C}\right) + q_{bc}^\alpha}{1 + \left(\frac{N_r}{1-f^{-1}}\right)^\alpha (1+\alpha)} \quad (4 \ 29)$$

where $N_r = N_C \sqrt{N_A}$. Thus what we need to know first hand is the values of C_F , \hat{N}_A ; other quantities are already known. They can be estimated from device structure. We note that too much accuracy in their values is not needed here as the modification (4 29) itself has little significance.

The next set of parameters I_k , β_F , I_{SE} and η_e remains essentially unchanged only the related equations are somewhat different. Note that in (2 104) we have introduced the quantity I_1 and I_2 where $I_1 = I_S/\beta_F$ and $I_2 = I_{SE}$. If we write $i_{cc} = i_r i_c(0) K_r$ where K_r is to be found out from (2 109) or (2 119) then the following equation can be derived

$$\frac{1}{h_{FE}} = \left| \frac{I_b}{I_c} \right| = \frac{q_b(0)}{K_r \beta_F} \sum_{n=1}^{\infty} k_n + I_{SE} \frac{(i_c(0) q_b(0))^{1/\eta_e}}{i_c(0) K_r} \sum_{n=1}^{\infty} k_{en} \quad (4 \ 30)$$

which is similar to (4 5). The way of deducing the values of K_r , k_n & etc. have already been described in Section 2 6. We also want to specify that $q_b(0)$ as a whole has to be calculated either from (2 63) or from (2 65). In them the part q_1 would be obtained from (4 29) and (2 37) while the part q_{20} by first determining τ_{fo} from (2 62) via (2 61) and (2 60) and then putting in (2 63) or in (2 65) in the latter case. The third way in tackling the problem which

we feel more convenient is to adopt lumped parameter model (Figure 2 13b) Here we take the simpler form (4 5) as our objective function The base series resistances taken would be R_b and R_b the latter one is to be determined from (2 113) or (2 114) or from (2 120) as the situation entails In q_b the part q_{bf} would be obtained from the prescript on suggested while dealing with the equation (2 122) or from (2 63) But in the latter case an average value of τ_{fo} has to be substituted

The third set of parameters re V_T I_S R_b and r_b For their evaluation the technique disclosed in Section 4 2 4 is recommended

The fourth set of parameters namely R I_{SC} η_c and $\tau_t (= \tau_f/\tau_r)$ would be identical to those in Section 4 2 5 if we take the definition of β_R as in (2 132) where the contribution of overlap diode D_1 automatically enters But if we accept the more sophisticated model (Figure 2 13b) then the presence of R_b separating the intrinsic part of the transistor from the overlap diode has to be considered The definition of β_R would then come on an equal footing with β_F i e the term containing i_b has to be deleted from (2 132) The set of equations those which will be relevant are (4 7) (2 13) (2 10) (2 126) (4 9) (4 10) (2 130) and (4 18) But because of the presence of the current I_{pd} the following modifications has to be made to the right hand side of these equations before we can use them: (a) subtract a term $I_{pd}R_b$ from (4 7) (b) add and subtract the current I_{pd} to

(2 13) and (2 10) respectively (c) add $I_{pd}(R_b + R_c)$ to
 (4 10) (d) replace V_{CB} by V_1 in (4 10) (e) subtract $(R_c/r_A)I_{pd}$

to the last of these equation the rest remaining unchanged

Note that we have chosen equation (2 130) instead of (2 64)

This set consists of eight equations with 10 unknowns The
 concerned parameters can be evaluated following the procedure
 adopted in Section 4 2 5

4 3 1 Extraction of Parameters on Base Push Out Effect

This requires separate attention as this effect
 appears in more than one set of measurements and the informa-
 tion laid in should be exploited for the simultaneous extrac-
 tion of the parameters We have mentioned in Chapter 2 Sec-
 tion 2 4 that the factor B in (2 63) should be replaced by
 $B = (w_{eff}/w_b)^2 = (1 + w_{CIB}/w_b)^2$ where appropriate expression
 for w_{CIB} is available from the set (2 75) - (2 77) as the
 situation demands By introducing the terms $r_w = w_{ep}/w_b$
 $j_s = q\mu_0 N_{ep} v_s$ $r_e = E_C/E_s$ V_{ep} $w_{ep} E_s$ The following
 results are derived from the above set of equations:

$$(a) \quad j_C \leq r_e j_s$$

$$B = \left[1 + r_w \left(1 - \frac{j_s}{j_C} \right) \frac{V_{BIC} - V_{BC}}{V_{ep}} \right]^2 \quad (4 31)$$

$$(b) \quad r_e j_s \leq j_C \leq j_s$$

$$B = \left[1 + r_w \left(\frac{j_s}{j_C} \right)^2 \frac{V_{BIC} - V_{BC}}{V_{ep}} \right]^2 \quad (4 32)$$

$$(c) \quad j_C > j_S$$

$$B = [1 + r_w \{1 - \frac{\epsilon v_S E_S^2}{V_{ep}(j_C - j_S)} (1 + \frac{2(V_{BIC} V_{BC})}{S E_S^2}) (j_C - j_S)^{1/2} - 1\}]^2 \quad (4.33)$$

Thus the parameters chosen are r_w , r_e , j_S and V_{ep} . Their initial values can be chosen from a knowledge of device structure and material properties the relationships being given in the first paragraph of this section. Since the factor B appears in both (4.6) and (4.20) the parameters evolved from one set of measurements are used as initial choice to the other set and this is done alternatively until convergence from either set is ensured.

4.4 COMPARISON WITH SPICE MODEL [35]

We have included this section with the view to make it (the proposed model) more convenient to the users for people are generally more familiar with SPICE model. In the modified form of SPICE as much as forty parameters are chosen. They are listed in Appendix III. There a separate column has been added to show the compatibility with the present proposition. Before going for any comparison we should mention that in the software package the name of the parameters τ_f , τ_t , I_S etc. are taken as TF , TT , IS ; the reason is obvious. Those which are identical are indicated by + sign. Those which are not same but can be a derivative of our model parameters the relationships are

indicated. Again SPICE program takes care of some more phenomena which we have not taken. As for example it has included the temperature dependence of I_s via the terms XTI and EG; the presence of n^+ junction capacitance (between the collector epilayer and the substrate) via CJS VJS MJS etc. They can also be incorporated straightway in the present model. It is found convenient to use expression for some variables instead of modelling them by more than one parameters. For example the variation in forward transit time τ_f has been taken care by introducing three additional parameters XTF VTF ITF in SPICE. However we are making use of an expression (2.62) for τ_f thereby avoiding the necessity of additional parameters. Hence fewer number of parameters are required in our version. Apart from this we have included some more effects like emitter edge crowding, mobility variation in the base region, base push out, conductivity modulation in low doped collector region etc. which have been simply ignored in the modified version of SPICE. It is also to be noted that our approach in tackling particular effects considerably differs (for example SPICE has accepted Hauser's expression [23] for modelling the modulation of base resistivity but we shall incline to use (2.114) or (2.120) for the same).

CHAPTER 5

SOFTWARE DEVELOPMENT

5 1 Introduction

In this chapter we will first briefly described the parent equations that are taken as objective functions of our optimisation problem. These equations are in fact already discussed in Chapter 2 and Chapter 4 but in a different forms. The reformulation of them is done as well as a different set of parameters is chosen with a view to attain greater numerical sensitivity. The complete flow chart and the program itself will be treated separately in Appendix IV. In section 5 2 experimental graph and data will be discussed whereas extracted output study will be the subject matter of the next section. In conclusion we shall indicate about the convergent criteria, the reasons for probable failures of the program in pathological cases and the way for their bypassing and remedies.

5 2 Objective Functions for the Simulation

The listing of the parameters of the simplified version of the model are: the eight parameters (P_e , P_c) related to junction depletion layer charges; saturation current I_g ; space charge currents I_{SE} , I_{SC} forward and

reverse ideal amplification factors β_F and β_R the forward transit time τ_F transit time ratio τ_t ($= \tau_F / \tau_R$) and forward knee current I_k required to model excess minority carrier charge in the base region; the four parameters r_w r_e j_s and v_{ep} related with base push out effect. Apart from them some more parameters resulting from the parasitics are also considered to get the terminal behaviours of the transistor

The important ones are R_b and $R_{b'}$ resistances of the active and inactive part of the base; R_c $R_{c'}$ resistance due to collector epilayer and that of the n^+ substrate; the parasitic capacitance C_{pe} between base and emitter contacts (as discussed in section 4.2.6) r_A the ratio of the active to inactive part of the collector junction; I_s the saturation current of the diode D_1 (see Fig. 2.13(b))

The four parameters P_e are related to V_{BIE} n_e C_{oe} and a_{e2} via equation (4.2) whereas the latter govern the junction capacitance C_e by (4.1). The way of extraction is indicated in that section (i.e. sec. 4.2.1). But from the optimisation solution point of view the equation is highly eccentric and crucked and the idea of extraction of four parameters may be sometimes misleading. Any way we take the logarithm of the expression and use the new set of parameters defined below so that the equation becomes

of less crucked nature

$$C_{oe1} = P(3) - P(2) \log V_{BEN} + \log \left(1 + \frac{(2)}{0.5 - P(2)} \frac{P(4)}{V_{BEN}} \right) \quad (5.1)$$

where $V_{BEN} = 1 + V_{BE} P(1) C_{oe1} \ln C_e$; the subscripted variable P is simulation parameter and not to be confused with P_e P_c listed above. Its elements are related as $P(1) = 1/V_{BIE}$; $P(2) = n_e/2$; $P(3) = \ln C_{oe}$ and $P(4) = a_{e2}$. In general fitting a set of points (C_{oe1}, V_{BE}) onto the theoretical expression would enable one extract the parameters P . We note from (5.1) that the expression is rather insensitive to the change of the value of $P(4)$; this may result in ill-conditioning of the coefficient matrix and extraction of parameter would generally become difficult. To get rid of this problem we recall that the parameter $P(4)$ comes in our way as a mean to avoid singularity in (2.19). Physically this models the presence of finite capacitance in forward bias when $V_{BE} \rightarrow V_{BIE}$. Hence if sufficient data in forward biasing conditions are taken the insensitivity can be minimised.

A similar description follows for the extraction of the elements of P_c . But here the value of $P(4)$ is very small and it is advisable to replace $P(4)$ by the constant value a_{c2} which can be estimated from an expression like (4.2).

The third set of parameters (V_T I_S R_{bb}) are identical to that listed in sec 4.2.4 the parent equation being 4.8. For this we have to have knowledge on q_b and h_{FE} . The appropriate values of the latter can be picked up from (h_{FE} I_C) measurement. For q_b we take its expression (4.6); in that q_{be} q_{bc} has to be found from (2.20) by using already known parameter from the last two runs. In the fourth term we put $B = 1$ and for the value of I_K we have to rely on experimental curve. It is advisable for extracting this set to take data points from low I_C V_{BE} portion of the curve. For this choice invalidates the approximation $B=1$ makes the magnitude of the fourth term in (4.6) insignificant so that an estimation of the value of I_K would not lead to any serious error and also the total base resistance $R_{bb} = R_b + R_b$ would be constant and a maximum since base resistivity modulation is absent. On the other hand too much low value of current should not be used as then the second term in (4.8) become insignificant and this may lead to difficulties in numerical analysis. Hence a compromise has to be made in choosing the data points.

Next we turn our attention to sec 4.2.2. For reasons already mentioned, we reformulated (4.5) as

$$h_{FEI} = P(1) q_b + \frac{P(2)}{I_C} (q_b I_C / I_S)^{P(3)} \quad (5.2)$$

and

$$\alpha_b = 1 + \alpha_{be} + \alpha_{bc} + \beta I_C P(4) \quad (5.3)$$

where the simulation parameters P 's are $P(1) = 1/\beta_F$, $P(2) = I_{SE}$, $P(3) = 1/\eta_e$, $P(4) = 1/I_K$ the parameter I_S is already extracted in the previous simulation. The parameters can be extracted as usual. Note that it is not h_{FE} but the reciprocal value has to be used as input to the program.

The measurement on R_E and R_{CC} is directly possible (see sec 4.2.3) and needs no simulation.

The parameters β_R , I_{SC} , η_C and τ_t (important while the CB junction is forward biased) are discussed in detail in section 4.2.5 for their simulation procedure. The parameters chosen for our programme are $P(1) = 1/\beta_R$, $P(2) = I_{SC}$, $P(3) = 1/\eta_C$, $P(4) = \tau_t$; the reason is obvious. Their initial values can be estimated from their expressions derived in Chapter 2.

The last set of parameters is on base push out effect evolved from simultaneous fitting then to (5.2) and (4.20) at high values of collector currents. This matter has been treated separately in section 2.4.2 and section 4.3.1 which is sufficient for the understanding

of the program By experience we have seen accepting value of $r_e (= E_C/E_S)$ from material properties rather than to use it as model parameter gives better numerical sensitivity

5 3 Results and Discussions

Our result and discussion would be based on the simplified version of the model yet enough accurate. The software developed is first tested by taking points from characteristic graphs supplied in the data book and then from measured values obtained during the course of the project work The end results are seen matching; some differences is also observed the reason for which is also predictable

In the page 117 of this book is shown a reprint of the relevant graphs of 2N2219A silicon NPN transistor from National Semiconductor Data Book [5] Out of them we have only used Fig 5 1(a) (b) (g) and (h) We have in fact faced a lot of problem while using them Since the graphs are conjusted the reading taken from them is not enough accurate and this leads to numerical problems It is seen while optimising the objective function the value obtained from simulation is matching with the input data to a degree higher than the degree of accuracy of the reading yet the program is not converging Secondly the set of graphs available is insufficient to record all the parameters As far as example graph 5 1(b) should be extended enough to give

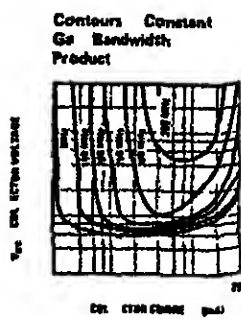
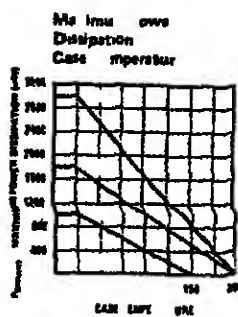
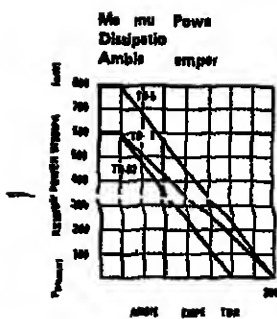
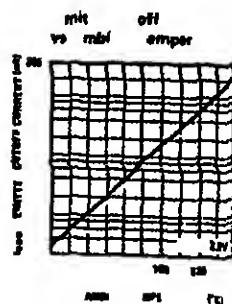
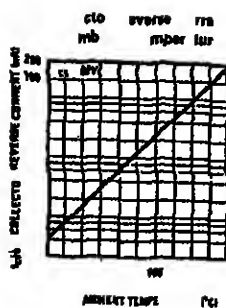
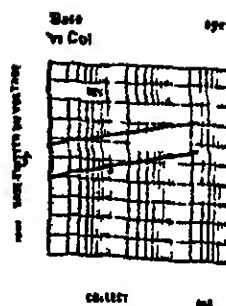
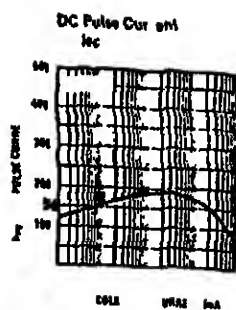


Fig 5 1 Characteristic curves of 2N2219A NPN transistor After [5]

an idea on knee current and knee voltage which are so important for setting initial choices in the program. The graph of output characteristics at saturation and at active region is also missing from the list. Anyway we have still used that because of its ready availability.

In the following table we will show data obtained from measurements. In Table 5.1 is shown data point extracted from EB and CB junction capacitance measurement. This is done by applying a ramp (slow enough to produce any charging and discharging current through the capacitance) superimposed by a small alternating voltage (~ 15 mV at 1 MHz). For this model PAR 410 ramp generator is used. To monitor the reading an XY plotter is connected which straightway plot the required graph. A digital voltmeter reads the voltages.

From the set of values of the extracted parameters we note a significant variation in their values for various set of measurements. Though convergence is achieved in all cases, the result shows the importance in choosing the region of data points. In Table 5.1() and Table 5.1() the data points are taken from forward bias region also and the result is more handsome and not contaminated. Before passing we would like to comment that the modelling of Early effect through punch through voltages etc. is more realistic and as it consumes less computer time it is acceptable for circuit simulation.

CV Measurement for EB and CB Junctions

Ramp applied:

Ramp rate = 10V/min

$V_{start} = 0.245V$ $V_{stop} = -5.71V$ (for EB junction)

$V_{stop} = -25V$ (for CB junction) $X_{scale} = 300 \text{ mV/cm}$

$Y_{scale} = 500 \text{ mV/cm}$ $C_{oe} = 21 \text{ pF}$ $C_{oc} = 9.1 \text{ pF}$

(a)

Ramp voltage	0 1	0 2	0 3	0 4	0 5	1 0	2 0	3 0	4 0	5 0
Capacitance $\ln(C_e)$	3 042	2 996	2 965	2 9392	2 912	2 7789	2 6246	2 5177	2 4248	2 3514

(b)

Ramp voltage	0 1	0 2	0 3	0 5	1 0	2 0	3 0	5 0	10 0	20 0
Capacitance $\ln(C_e)$	2 1804	2 1041	2 0605	1 96	1 8563	1 7138	1 639	1 5369	1 3737	1 1939

(c)

Ramp voltage	-	2512	0 0	2512	5023	7534	1 130	1 632	2 512	3 516	4 7716
Capacitance $\ln(C_e)$	3 183	3 054	2 961	2 891	2 84	2 769	2 702	2 605	2 527	2 451	

Continued

TABLE 5 1 (Continued):

3)

amp	0 0	1622	4595	7295	9189	1 2703	1 9189	2 9189	3 7838	4 5946
Itage										
apacitance	2 2192	2 1278	2 0033	1 9204	1 8694	1 7951	1 709	1 59	1 5163	1 464
n(C _c)										

Table 5 2

h_{FE} V_{BE} vs I_C at Constant V_{CE} (10 v)

I_C in m_A	0 1	0 2	0 3	0 4	0 5	1 0	2 0	3 0	4 0	5 0
h_{FE}	120	130	136	142	145	150	155	168	175	180
V_{BE} at 373 K	0 4	0 425	0 437	0 445	0 45	0 475	0 492	0 502	0 510	0 542
V_{BE} at 300 K	0 572	0 590	0 601	0 609	0 618	0 630	0 638	0 655	0 665	0 672

The next table shows points taken from both the data sheet and that through measurement. Along with the values we have also indicated the room temperature over which the measurements are taken. It is important to note the variation of V_{BE} with temperature at same collector current. The corresponding table for extracted parameters are also indicated.

Table 5 3
Capacitance Parameters Values

Parameter name	Table 5 1(a)	Table 5 1(b)	Table 5 1(c)	Table 5 1(d)
V_{BIE}	8398E+00	2005E+00	6142E+00	3652E+00
$1/n_E$	3757E+00	2289E+00	2850E+00	3051E+00
C_{Oa}	2093E+02	9639E+01	1963E+02	7995E+01
a_{e2}	1130E+00	1681E-05	3436E+00	6468E+00

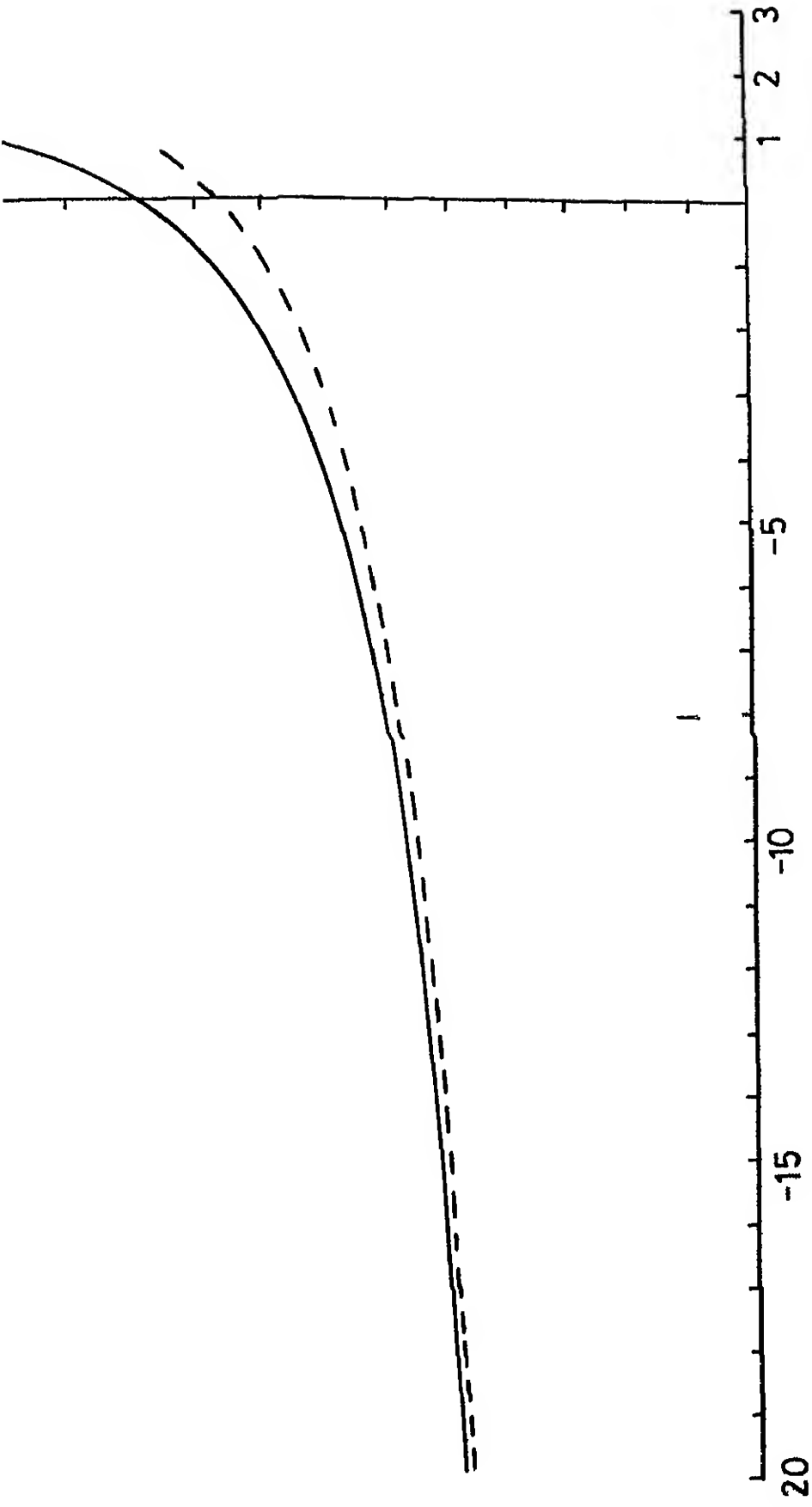
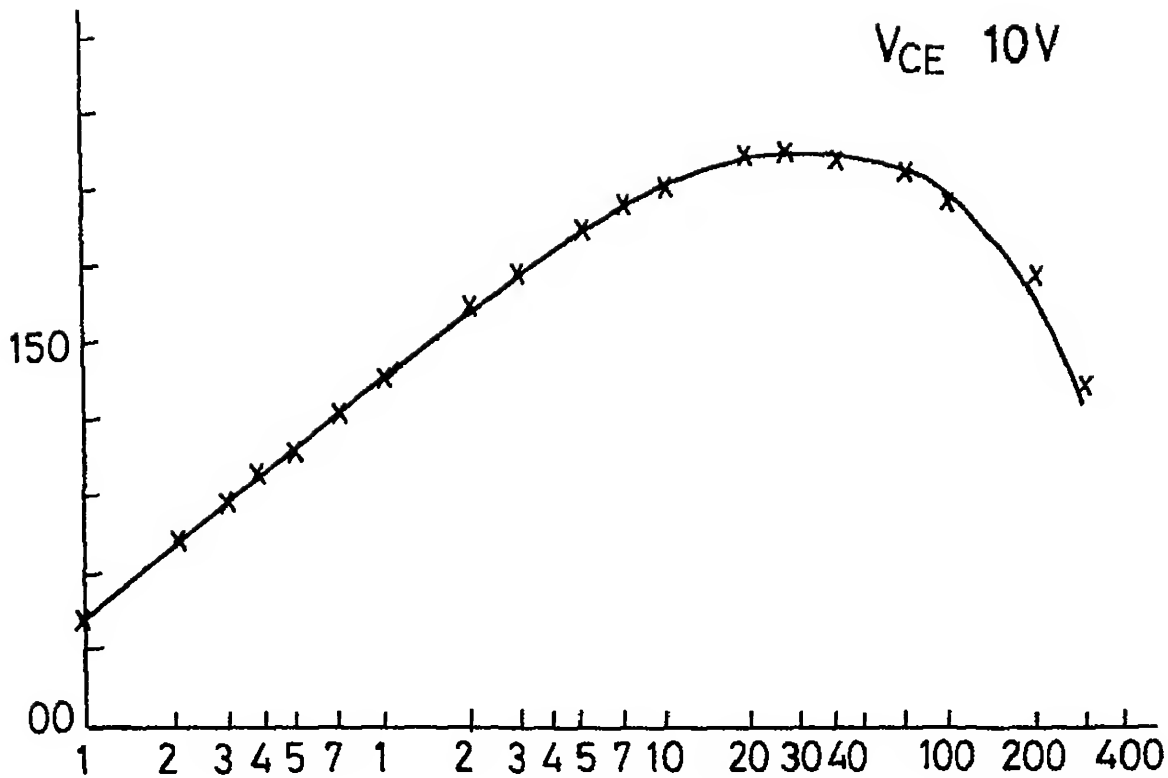
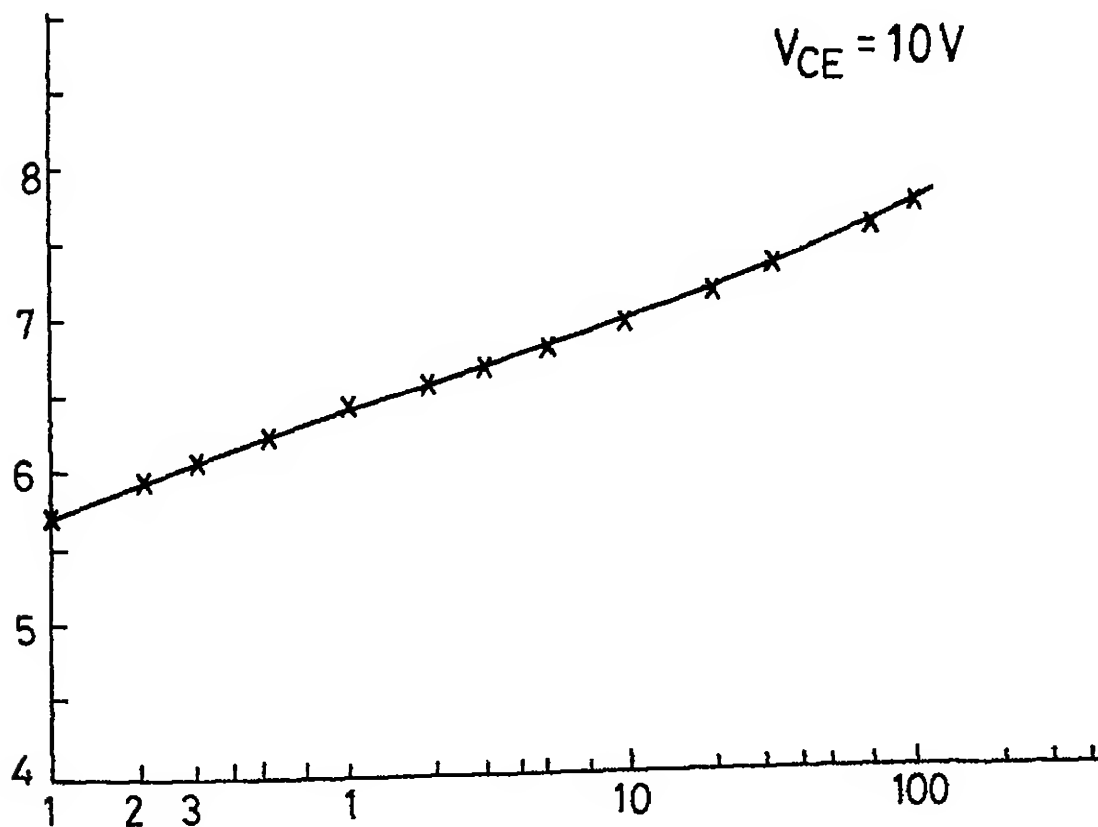


Fig 52 CV curves in reverse biases The continuous one is for
CB junction, vertical scale, 1 div=1 pF, the dashed one for
EB junction, vertical scale 1 div=25 pF, while the horizontal
scale is in volts

$V_{CE} = 10V$  $V_{CE} = 10V$ 

5 3(a) h_{FE} Vs I_C at constant V_{CE} (b) V_{BE} Vs I_C
at constant V_{CE}

CHAPTER 6

CONCLUSION AND SUGGESTIONS FOR FURTHER WORK

In this work a unified approach for modelling bipolar junction transistor of either type from large signal dc analysis has been presented. The basic premises of all the model expressions is from Gummel's charge control theory. All most all known major non-linear effects have been incorporated and appropriate reformulation is done when one or more secondary effects are present in particular region of operation of a transistor. As for example and high injection both conductivity modulation and emitter edge crowding are present one inducing the other and they have been accommodated collectively. We have indicated the way to choose tacitly the data points for the extraction of a particular set of parameters and the initial choice of parameters. This is extremely important from simulation point of view and as also the expressions are quite nonlinear in nature. The situation in deep saturation and inverse active mode operation is generally more complex and the assumptions to be taken as a basis for modelling this region seems to be more stringent than that in forward active and saturation mode. We have taken enough care for extrapolation of the previous set of expressions.

The validation of the proposed model (extended GP) has not been done in the present work. We have tested only the simplified version. The required experimental set up and the way to take various measurements has been proposed. By taking the appropriate measurements the software of the program could be developed. Some of the effects which we have not included can be easily added as for example the presence of collector depletion region to substrate capacitance, temperature dependence of I_s etc. There are many more facets of the device that one may be interested in but it is hoped that the above suggestions if implemented is sufficient for any practical purpose. The software package so developed may be used as a module for simulating circuit behaviours.

BIBLIOGRAPHY

- 1 Linear data book National semiconductor (1982)
- 2 The TTL Data Book Texas Instruments (I)
- 3 Microelectronics (CH 16 & 17) Jacob Millman McGraw-Hill Book Company (1979)
- 4 Advanced Electronic Circuits U Tietze & Ch Schenk
- 5 Transistor Data Book - National Semiconductor (1980)
- 6 Ebers J J and Moll J L Large-Signal Behaviour of Junction Transistors Proc IRE 42 No 12 (Dec 1954) pp 1761-1772
- 7 Gummel H K and Poon H C An Integral Charge Control Model of Bipolar Transistors Bell Syst Tech J Vol 49 (May 1970) p 827
- 8 Moll J L and Ross I M The Dependence of Transistor Parameter on the Distribution of Base Layer Resistivity Proc IRE Vol 44 (Jan 1956) pp 72-78
- 9 Poon H C and Mechwood J C Modelling of Avalanche Effect in Integral Charge Control Model IEEE Trans on ED Vol 19 (Jan 1972) pp 91-97
- 10 Poon H C Modelling of Bipolar Transistor Using Integral Charge Control Model with Application to Third Order Distortion Studies IEEE Trans on ED Vol 19 (June 1972) pp 719-731
- 11 Sah C T Noyce N and Shockley W Proc IEEE (Lett) Vol 57 (Dec 1969) p 2181
- 12 Fletcher N H Self bias Cut off Effect in Power Transistor Proc IRE Vol 43 (Nov 1955) p 1669
- 13 Webster W M On the Variation of Junction Transistor Current Gain Amplification Factor with Emitter Current Proc IRE Vol 42 No 6 (June 1954) p 914
- 14 Kirk C T A Theory of Transistor Cutoff Frequency (f_T) Fall-off at High Current Density IEEE Trans on ED Vol 9 (March 1962) p 164
- 15 Gray P E et al Physical Electronics and Circuit Models of Transistors SSEE Vol 2 Wiley New York 1966

- 16 Gandhi S K Semiconductor Power Devices Wiley
New York 1977
- 17 Getreu I E Modelling the Bipolar Transistors
Elsevier New York 1978
- 18 Daw A N Mitra R N and Choudhury N K D Cut-
off Frequency of a Drift Transistor Solid State
Electron V 10 (1967) p 359
- 19 Polsky B S and Rimsham J M 2-D Numerical Solution
of BJT Taking into Account of Heavy Dop ng Effects and
Fermi Statistics Solid State Electron Vol 26 No 4
(April 1983) p 275
- 20 Jean and Markos A New Formulation of Early Effect in
Epitaxial BJT Solid State Electron Vol 27 No 6
(June 1984) p 519
- 21 Rein H M Proper Choice of Measuring Frequency for
Determining f_T of BJT Solid State Electron Vol 26
No 1 (Jan 1983) p 75
- 22 Roulston D J IEEE Trans on ED Vol 19 No 6 (June
1972) p 809
- 23 Hauser J R The Effect of Distributed Base Potential
on Emitter Current Injection Density and Effective R_{bb}
for Stripe Transistor Geometries IEEE Trans on ED
Vol 11 (May 1964) p 238
- 24 Unwin R T and Khott K F Comparison of Method for
Determining R_{bb} IEE Proc Part I Vol 27 No 2
(April 1980)
- 25 Lary and Anderson Effective Base Resistance of BJT
IEEE Trans on ED Vol 32 (Nov 1985)
- 26 Filensky W and Beneking J New Techniqucs for
Determination of Static Emitter/Collector Series
Resistance of BJT IEEE Electron Lett Vol 17
(1981) p 504
- 27 Graaff and Kloosterman IEEE Trans on ED Vol 32
No 11 (Nov 1985) p 2415
- 28 Prichard R L Two Dimensional Current Flow in
Junction Transistor at High Frequencies
- 29 Mohankrishnan N High Injection Modelling of a
Junction Transistor M Tech Thesis I I T Kanpur
July 1977

- 30 Tyagi M S Physics of Semiconductor Devices
Unpublished
- 31 Gummel H K A Charge Control Relation of BJT Bell
Syst Tech J Vol 49 (1970) p 115
- 32 Sridharrao W C M Tech Thesis I I T Kanpur (1970)
- 33 Nussbaum Allen The Theory of Semiconductor Junction
CH 2 Monographs on Semiconductors and Semimetals Ed
R K Willardson and A C Beer Vol 15 Academic Press
(1981)
- 34 Rey G et al A Unified Approach to the Base Widening
Mechanism in Bipolar Transistors Solid St te Electron
Vol 18 (1975) p 863
- 35 SPICE Version 2G Dept of EE & CS Univ of Calif
Berkeley
- 36 Das A K 'Computer Aided Parameter Extraction of
MOSFETS M Tech Thesis I I T Kanpur (1985)
- 37 Early J M Effects of Space Charge Layer Widening in
Junction Transistors Proc IRE Vol 40 (Nov 1952)
- 38 Schott & Roulston Solid State Electron ibid
(1982)
- 39 Poon H C and Gummel H K Modelling of Emitter
Capacitance Proc IEEE (Lett) Vol 57 (Dec 1969)
p 2181
- 40 Gummel H K Hole Electron Product of a P N Junction
Solid State Electron Vol 10 (1967) p 209
- 41 Gummel H K On the Def nition of Cut-off Frequency
Proc IEEE (Lett) Vol 57 (Nov 1969) p 2159
- 42 Shockley W et al p n Junction Theory Phys Rev
Vol 83 (July 1951) pp 151-162
- 43 Solomon J E The Monolithic OPAMP A Tutorial Study
IEEE Trans on Solid State Circuits Vol 9 No 6
(Dec 1974)

APPENDIX-I

BALANCING TECHNIQUES FOR OFFSETS OF OPAMPS

An ideal operational amplifier is perfectly balanced that is when $V_1 = V_2$ $V_o = 0$. A real operational amplifier exhibits an unbalance caused by a mismatch of the input transistors also because of temperature grading effect [43]. This mismatch causes unequal bias currents (i_B^+ and i_B^- respectively) flowing through the input terminals and also an input offset voltage V_{io} which must be applied between the input terminals to balance the amplifier.

A modified form of the equivalent circuit is shown in figure (1a). Here we have taken instead of i_B^+ and i_B^- the input bias current $i_B = (i_B^+ + i_B^-)/2$ and input offset current $i_{io} = i_B^+ - i_B^-$ when $V_o = 0$.

Consider the case when the OPAMP is active in inverting mode. With positive input terminal grounded, there exists a virtual short circuit between the input terminals. Hence whole of the current i_B^+ flows through R_f creating a voltage drop $i_B^+ R_f$. Again if there exists only the dc offset voltage V_{io} with positive terminal grounded, V_{io} appears across R resulting in a current V_{io}/R . The same current flows through R_f . Hence the output voltage $V_o = (R + R_f) V_{io}/R$. Applying superposition we see that the net output voltage appears to be

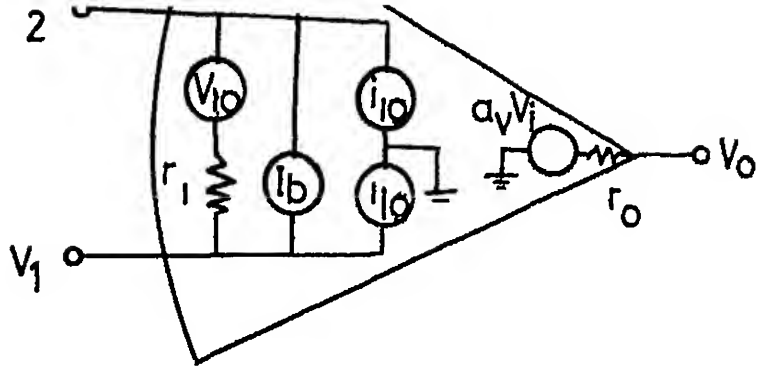
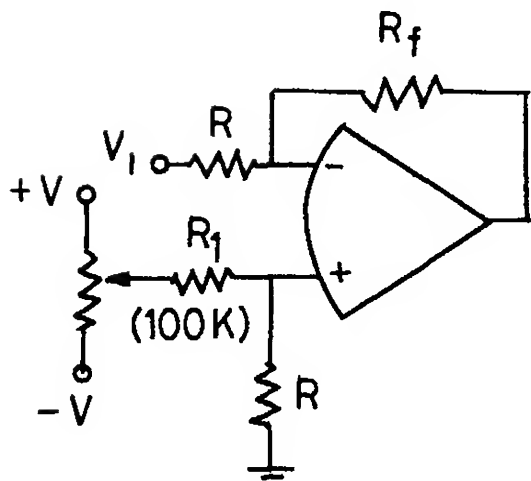


Fig 1(a)



g 1(a) dc equivalent circuit of an OPAMP
 (b) Universal offset balancing
 technique in inverting mode [3]

$$V_o = i_B^- R_F + V_{io} (1 + R_F/R) \quad (A 1)$$

In case offset currents i_B^+ and i_B^- are either known or measured the contribution due to offset current can be fully annulled by placing a resistor R in the positive terminal so that $i_B^+ R - i_B^- R_{||} (R = R || R_F)$. But if they are not known then choose $R = R_F$ so that at least the effect due to bias current i_B is nullified leaving behind a small output error $V_o = -i_{io} R_F$. The offset voltage effect is offsetted by using the potentiometer as shown in figure I(b). It allows a small voltage effectively in series with the noninverting amplifier in the range $\pm V R / (R_1 + R)$. Choice of R is as already discussed in connection with reducing offset current effect. Since $R_1 = R$ the offset voltage circuitry is amply isolated and thus the two effects are controlled independently. The balancing technique can similarly be considered for non-inverting mode operation.

APPENDIX-IICB JUNCTION WIDTH AS A FUNCTION OF VOLTAGE

We start with the one dimensional Poisson equation

$$-\frac{d^2V}{dx^2} = \frac{dE}{dx} = \frac{\rho(x)}{\epsilon} = \frac{q}{\epsilon} [p(x) - n(x) + N_d(x) - N_A(x)] \quad (\text{II } 1)$$

and apply it over the depletion region to the either side of the CB junction. To the base side $N_d(x) - N_A(x) - N_{ep}(1 - e^{-C_F x})$ and to the collector side it is N_{ep} only. If we assume the mobile carriers of the transported current moves with the saturation velocity v_s in the depletion region due to the presence of high electric field then their number ($= j_c / q v_s = N_{ep}(j_c / j_s) = N_{ep} j_{cn}$ (say) where j_s is defined in (4.3.1) ought to be added to the base side and to be subtracted from the collector side. Neglecting the majority carrier contribution in the depletion region we get the equations for the respective regions as

$$\frac{dE}{dx} = - \frac{q N_{ep}}{\epsilon} (e^{-C_F x} - 1 + j_{cn}) \simeq - \frac{q N_{ep}}{\epsilon} (e^{-C_F x} - j_{cn}) \quad (\text{II } 2)$$

$$\frac{dE}{dx} = + \frac{q N_{ep}}{\epsilon} (1 - j_{cn}) = \frac{q N_{ep}}{\epsilon} j_{cn} \quad (\text{II } 3)$$

where $j_{cn} = 1 - j_{cn}$. The boundary values for the electric field is $E = E_m$ at $x = 0$, $E = C_F V_T$ at $x = -x_p$, $E = E_{cz}$ at $x = x_n$ where

x_n and x_p are the depletion width to the base and collector side respectively. Using these boundary values (II 2) and (II 3) can be solved to yield

(a) For $-x_p \leq x \leq 0$

$$E(x) = - \frac{qN_{ep}}{\epsilon} \left[\frac{e^{C_F x_p} - e^{-C_F x}}{C_F} - j_{cn} (x + x_p) \right] + C_F V_T \quad (\text{II } 4)$$

(b) For $0 \leq x \leq x_n$

$$E(x) = - \frac{qN_{ep}}{\epsilon} (x - x_n) j_{cn} - E_{cz} \quad (\text{II } 5)$$

where

$$E_{cz} = j_{cn} v_s / \mu_0 \quad (\text{II } 6)$$

The maximum electric field is given by

$$\begin{aligned} E_m &= - \frac{qN_{ep}}{\epsilon} \left(\frac{e^{C_F x_p} - 1}{C_F} \right) + C_F V \\ &\approx - \frac{qN_{ep} j_{cn}}{\epsilon} x_n - E_{cz} \end{aligned} \quad (\text{II } 7)$$

This gives the first relationship between x_n and x_p . We note that the linking current reduces the maximum electric field. Equality (II 7) is an approximate one because of presence of j_{cn} ; E_m does not exactly occur at $x = 0$. Any way for low current (when no base push out effect) (II 7) is sufficiently accurate.

The total voltage drop $v_{BIC} - v_{BC} = - \int_{-x_p}^{w_{ep}} E(x) dx$;

if we break up the integration limits from $-x_p$ to 0 0 to x_n then x_n to w_{ep} and use expressions (II 4) (II 5) and (II 7) in the respective regions we will land down with

$$V_{BIC} - V_{BC} = E_m (x_p - 1/C_F + \frac{1}{2} x_n) - \frac{1}{2} j_{cn} x_p^2 - C_F V_T x_p + E_{cz} w_{ep} \quad (II 8)$$

The charge conservation across the junction gives us

$$\frac{C_F x_p - 1}{C_F} = \int_{-x_p}^{x_n} (1 - \frac{n_e(x)}{N_{ep}}) dx \quad (II 9)$$

where $n_e(x)$ would be given by (for $j_{cn} < r_e$) where r_e is defined in Section (4 3 1)

$$n_e(x) = \frac{j_n}{\mu_o E(x) + V_T d/dx (\ln(x))} \quad (II 10)$$

where $n_e(x)$ is to be solved by NR technique with boundary

values as at $x = -x_p$ $n_e(x) = \alpha n(0)$ $n(0)$ being the

charge injected from the EB junction and $E(x_p) = C_F V_T$

At the other end $n_e(x) = N_{ep}$ and $E(x_n) = -E_{cz}$ Now the

built in electric field V_{BIC} is given by

$$V_{BIC} = V_T (x_p/C_F + 2 \ln N_{ep}/N_1 - 1) \quad (II 11)$$

where the last term in this expression is introduced to account for majority carrier effect in the base side The

relationships (II 8) to (II 11) helps us determining x_n and x_p as a function of voltage. To solve this equation first assume $x_p = 0$ and solve for x_n . With the value of x_n so obtained the same set of equation is solved for x_p .

[illegible]

Extraction of GP Parameters

